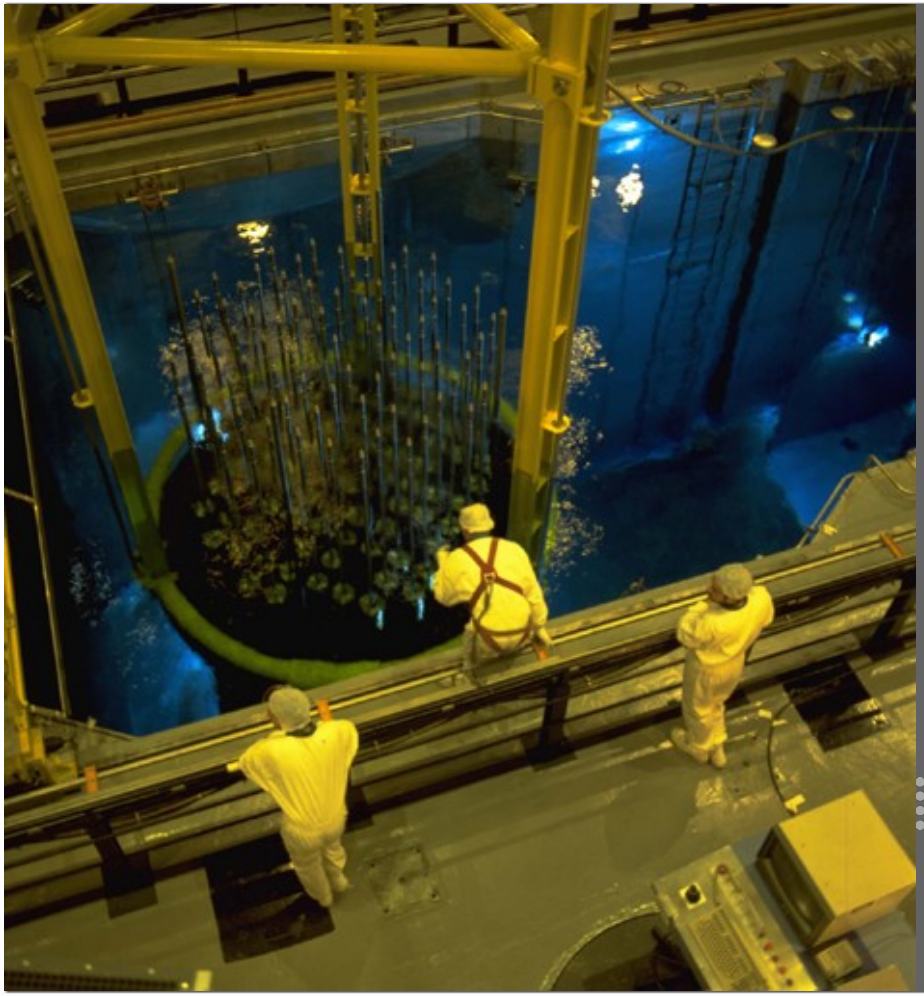

The Kinetic Monte Carlo method

Pär Olsson
KTH Royal Institute of Technology
Nuclear Engineering
polsson@kth.se

Origin of Monte-Carlo methods

- **Monte-Carlo** refers to a broad class of algorithms that solve problems using random numbers.

- The stochastic method has existed since well before the first computer and was e.g. used by Enrico Fermi in 1930.

- One useful instance is the Metropolis algorithm* which allows by very simple means to find the equilibrium state of a system.

*N. Metropolis et al, J. Chem. Phys. 21 (1953) 1087.

Origin of Monte-Carlo methods

Applications range from:

- Graphic ray tracing
- Semiconductor Carrier simulation
- Financial analysis
- Numerical integration
- Neutron transport
- Diffusion in solids
- etc…

Origin of Monte-Carlo methods

Metropolis Monte-Carlo:

Classically: Transmutation MC, switching of particles

Switch acceptance based on the probability ratio between initial (ij) and final (ji) state:

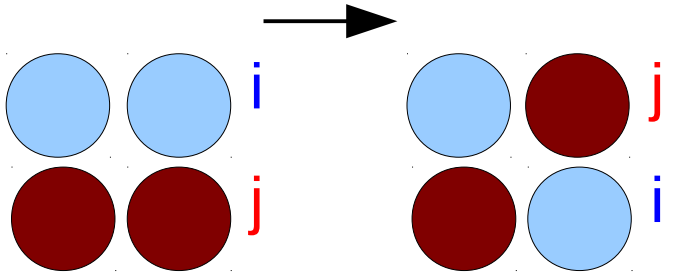

If $P_{ij \rightarrow ji} = exp(-\Delta U / k_B T) > 1$ then accept,

If not, accept with probability $P_{ij \rightarrow ji}$

where ΔU is the potential energy difference between the states ij and ji.

Origin of Monte-Carlo methods

Metropolis Monte-Carlo:
Efficient algorithm for finding equilibrium configurations.
“Path” to final state without physical meaning.
No information on the time scale.

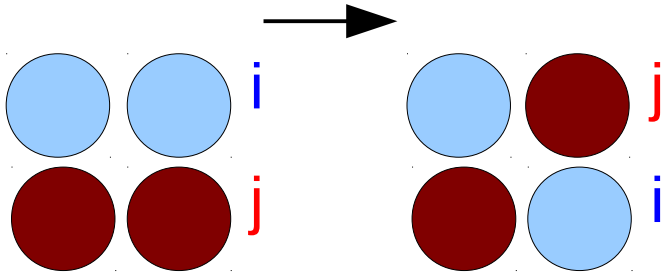

However, coupled with cohesive model, provides path to thermodynamic integration (if atomic relaxation is allowed).

Time for Kinetic Monte-Carlo

Question: How do we treat the time evolution of systems defined by diffusion processes?

Diffusion: Generally activated by jumps over energy barriers:

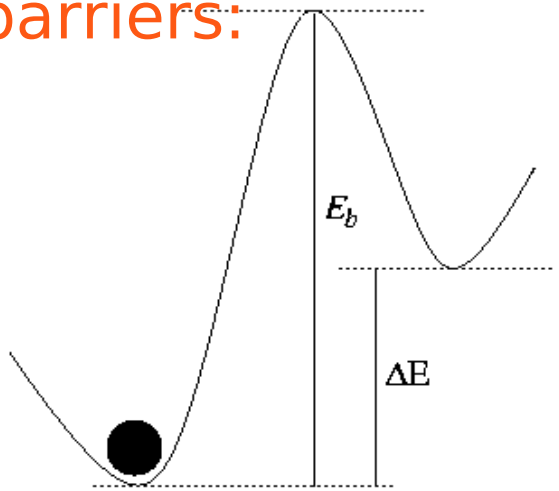

barrier to higher energy state

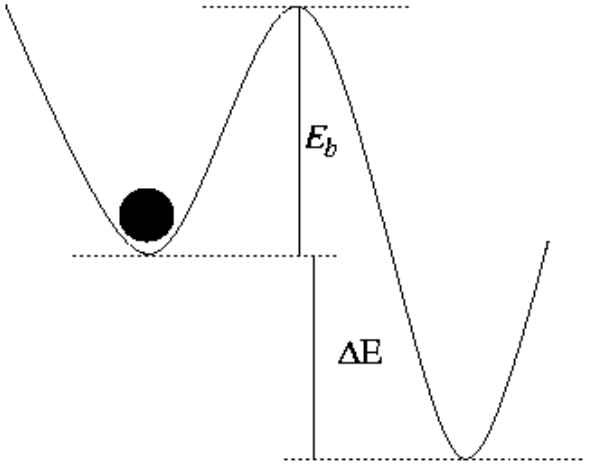

barrier to lower energy state

e.g. thermal activation: $$R(T) = R_0 e^{-E_b/k_B T}$$

Time for Kinetic Monte-Carlo

Surface: Hopping, exchange, adsorption, desorption, etc

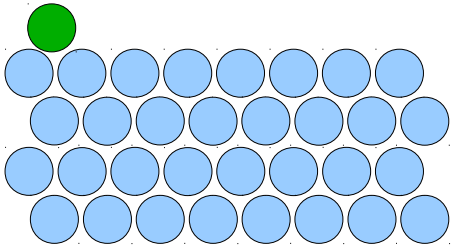

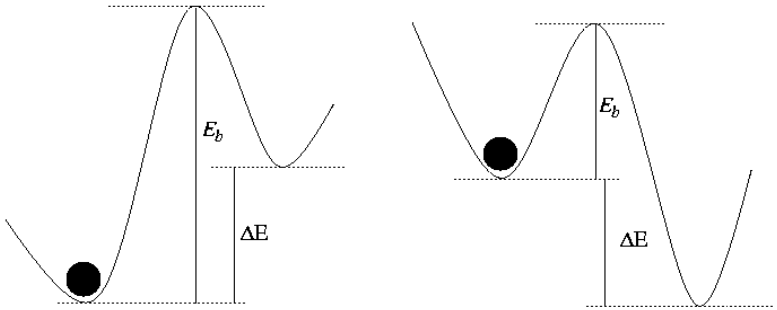

$$R(T) = R_0 e^{-E_b/k_B T}$$

Bulk: Vacancy driven, self-interstitial driven, diffusion of interstitial elements.

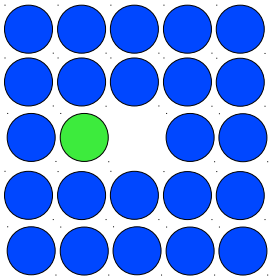

Time for Kinetic Monte-Carlo

How to advance the system: $R^i(T) = R_0^i e^{-E_b^i/k_B T}$

1) Use short time step Δt. For each step go trough all particles *i* and randomly choose according to R^i if a process is activated.

Limit: $\Delta t << 1/R_{max}$ → very slow algorithm if rates are strongly varying

2) Pick a particle *i* at random, with probability proportional to R^i. Every step produces a jump; time step association easy.

The KMC method!

Outline

1. Introduction
   - Origin of Monte-Carlo methods
   - Time for Kinetic Monte-Carlo
2. Kinetic Monte-Carlo method
   - Physical motivation
   - Mathematical formalism
   - Numerical recipie
   - Range of applicability
   - Advanced methods
3. Applications
   - Atomistic KMC – thermal ageing & microstructure evolution
   - Object KMC – resistivity recovery

KMC – History

Atomistic Monte-Carlo: The Metropolis algorithm (1953)

No timescale!

Kinetic Monte-Carlo: ?

1) Flinn and McManus, Phys. Rev. 124 (1961) 54.

Vacancy driven but no explicit time

2) Young and Elcock, Proc. Phys. Soc. 89 (1966) 735.

Simple time scale

3) Bortz, Kalos and Lebowitz, J. Comp. Phys. 17 (1975) 10.

Ising sping KMC with rigorous time scale (no reference to Young and Elcock...)

KMC – History

Kinetic Monte-Carlo:

The algorithm derived in the BKL paper is usually called the *residence time algorithm* (you will see why), also called the *n-fold way*, the *BKL method*, or more generally the KMC method.

Modern reviews:

Fichtorn and Weinberg, J. Chem. Phys. 95 (1991) 1090.

Voter, in Radiation Effects in Solids, (Springer, NATO Publishing Unit, Dordrecht, The Netherlands, 2005)

KMC – Physical motivation

Many interesting processes consist mainly of diffusive jumps from one state to another.

Skip vibrational dynamics and go for the heart of the problem: The state-to-state transitions.

Normally the transition from one basin to another is an infrequent event, i.e. $t_{\text{in basin}} >> t_{\text{transition}}$

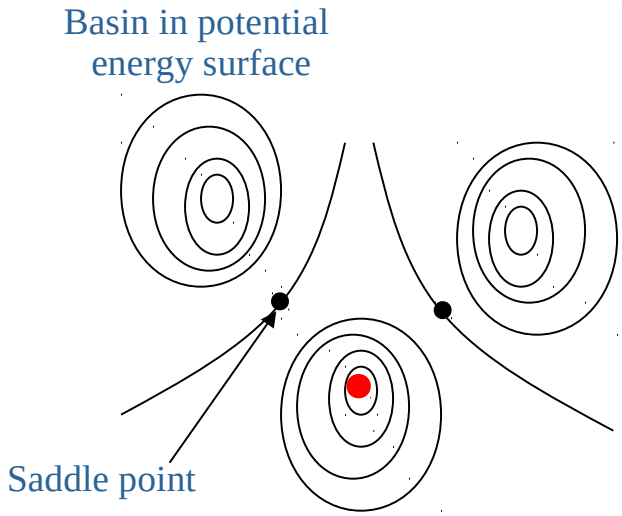

Thus the memory of how each transition transpired is lost. All transitions are independent of the system history.

KMC – Physical motivation

Thus, for each transition from one basin i to another j, there is a rate constant r_{ij} that characterizes the probability to escape from i to end up in j.

No dependency on state i-1 exists:

→ a Markov chain.

If all $\{r_{ij}\}$ are known, the system trajectory will be indistinguishable from that of a fully dynamic simulation.

MD

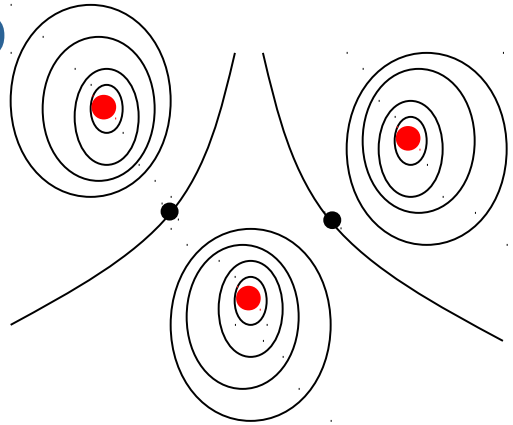

KMC

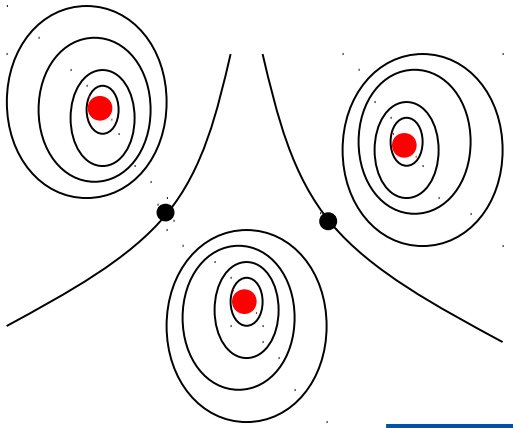

KMC – Physical motivation

Due to the memory loss of the system, the probability of transition is identical for all equal (and short) time steps t.

⇨ a process with first-order decay statistics (Poisson process), e.g. radioactivity.

The probability of the system staying in a certain basin is:

$$P_{stay}(t) = \exp(-r_{tot}t),$$

where r_{tot} is the total rate for escape from the particular state.

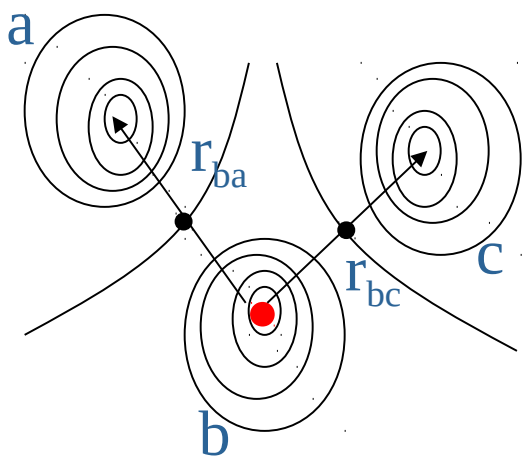

$$r_{tot} = r_{ba} + r_{bc}$$

KMC – Physical motivation

Requirements:

a) The transitions are Poisson processes
b) The processes are independent
c) The time increment is calculated properly

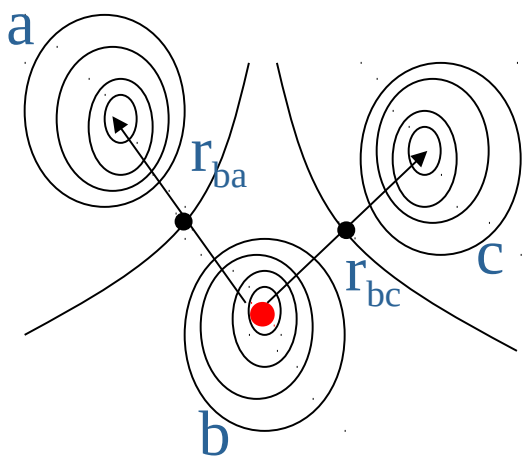

$$r_{tot} = r_{ba} + r_{bc}$$

KMC – Numerical recipie: meta code

0. Set time t=0.
1. Form a list of all rates r_i of all possible transitions W_i in the system.
2. Calculate the total rate $R_i = \sum_j^i r_j$ for i = 1,...,N where N is the total number of transitions.
3. Get a uniform random number c ∈ (0,1].
4. Find the event *i* corresponding to c: $R_{i-1} < cR < R_i$
5. Carry out event *i*.
6. Find all W_i and recalculate all r_i that may have changed.
7. Get a new uniform random number c ∈ (0,1].
8. Update the time with t = t + Δt where:
9. Return to step 1.

$$\Delta t = -\frac{ln(c)}{R}$$

KMC – Numerical recipie

How to calculate the rate constants?

Transition state theory gives us a straightforward scheme:

r_{ij} is given by the equilibrium flux through the surface separating the two states (the saddle point).

This can be simulated using e.g. the Metropolis algorithm.

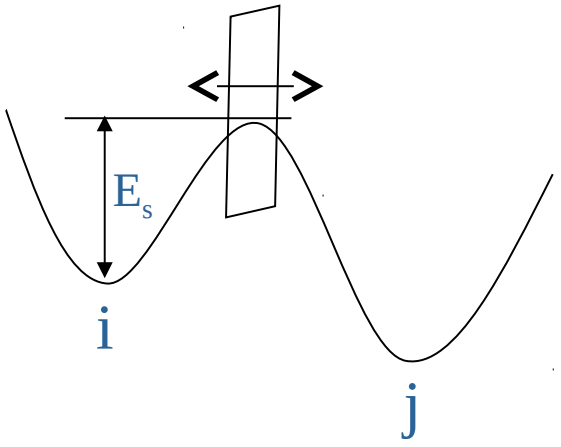

However, to further simplify, we can assume a harmonic transition state.

KMC – Numerical recipie

Harmonic transition state theory (Vineyard theory).

Only allows passage through the saddle point.

Vibration modes around the saddle point are harmonic.

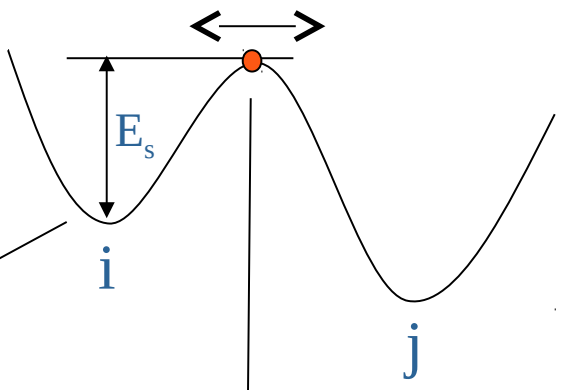

normal modes @ min

$$r^{\mathrm{TST}} = \frac{\prod_i^{3N} \nu_i^{\mathrm{min}}}{\prod_i^{3n-1} \nu_i^{\mathrm{sp}}} \exp\left(-\frac{E_s}{kT}\right)$$

normal modes @ sp

Transition rates – drag method

Choose appropriate reaction coordinate q

Constrain q and relax all other degrees of freedom

Repeat procedure for several q between initial and final state

- highly dependent on good guess for reaction coordinate
- if true reaction coordinate has a large component perpendicular to the initial guess, the method will yield a discontinuous reaction path!

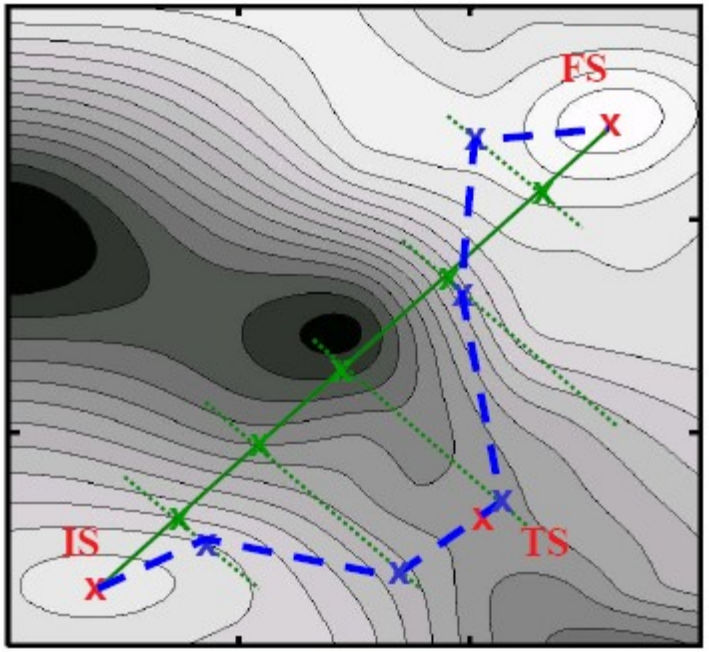

Image from Peter Kratzer

Transition rates – NEB method

Nudged elastic band:

Initialize with several images $\{R_i\}$ along a straight-line interpolation

Minimize

Problem:

$$S(R_1, ..., R_N) = \sum_i E(R_i) + \sum_i \frac{k}{2}(R_{i+1} - R_i)^2$$

- elastic band cuts corners
- images tend to slide down towards low-energy IS/FS regions, leaving few images for relevant TS region

Solution:

- only spring force component parallel to path (no corner cutting)
- only true force component perpendicular to path (no down-sliding)

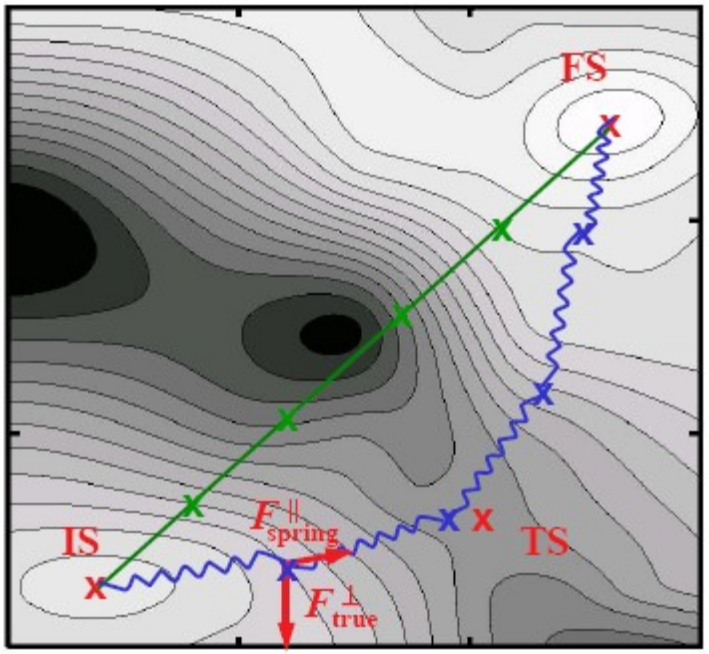

G. Mills and H. Jónsson, Phys. Rev. Lett. **72**, 1124 (1994)

Image from Peter Kratzer

KMC – Range of applicability

KMC does give a trajectory identical to a fully dynamic simulation if (and only if) the rate catalogue is *complete*.

In simple cases (1D, etc) this condition might be fulfilled but in complex systems like 3D solids or surfaces it is *not* trivial!

If only our intuition is allowed to define the rate catalogue we will miss processes.

The question is how important they are…

KMC – Range of applicability

Example from Voter: Adatom exchange on fcc(100) [Pt, Ir, Al]

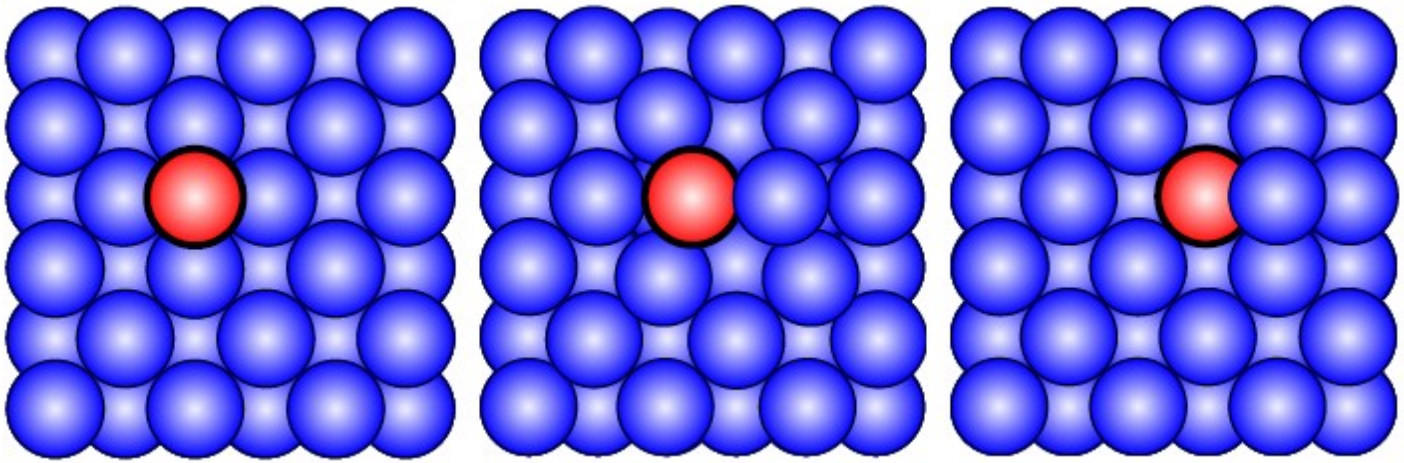

Exchange mechanism discovered by DFT (Feibelman 1990)

Previous studies assumed surface hopping: simulations not in agreement with experiments.

KMC – Range of applicability

Computational scaling

Depends on:

the size N of the rate catalogue.

which in turn depends on the system size unless the density of "jumpers" is not constant.

Special cases exist where computation time is independent on N.

Below-N scaling is possible using binning methods and recursive tree searches.

Place all events with rate r_i into bin j

Select events by first choosing bin, then randomly inside the bin.

Scales as log(N)

Maksym, Semicond. Sci. Technol. 3 (1988) 594.

KMC – Range of applicability

Advantages:

Simulated objects can change character:

- reactions introducing new reaction products
- annihilation/recombination
- emission

The r_{tot} is updated all the time: time scale varies with population

Fast moving population evolving into slow moving population dynamically changes the time scale.

Several orders of magnitude in time can be treated in one simulation!

- initially: $\Delta t \sim$ fs, finally: $\Delta t \sim$ h

KMC – Range of applicability

Disadvantages:

All rates and reaction have to be known.

Method cannot predict new reactions!
(unlike MD)

Exp/ab initio/MD can give rates and reactions.
(complex combinatorics, model simplifications, etc)

KMC lab next!

Parallel KMC

How do we reach longer time scales or larger simulation boxes?

"Standard" solution: parallelize the problem. Decompose the domain and share the load between processors.

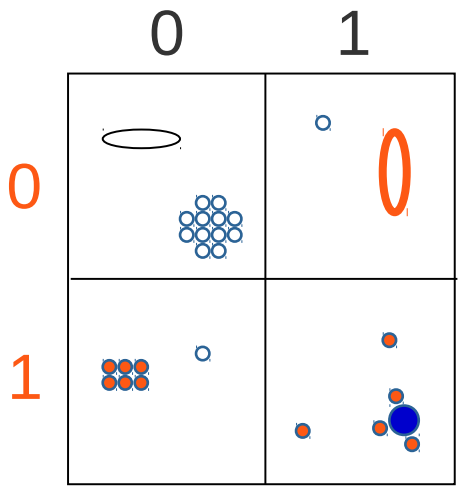

One processor per domain, speedup is determined by degree of communication (surface/volume ratio).

Parallel KMC

but... KMC is an inherently sequential method.

Take a simulation box with a number of objects and a simple spatial domain composition:

In each domain (00,01,10,11) the time step depends on the characteristics of the simulated event.
e.g: A single vacancy jump differs from an interstitial loop recombination.

Thus, the time advance in each region is asynchronous. When objects cross into neighbouring domains, the times have to match.

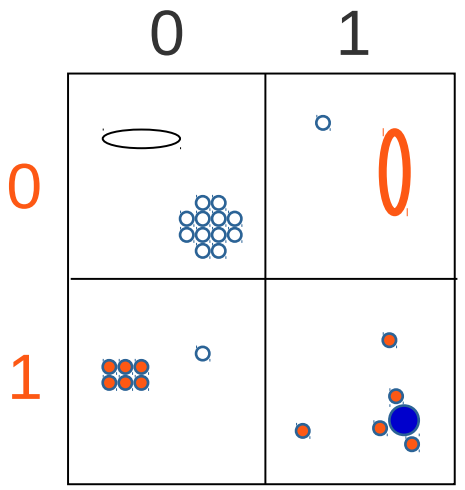

$$\Delta t_{00} \neq \Delta t_{01} \neq \Delta t_{10} \neq \Delta t_{11}$$

Parallel KMC

Some ways around the problem:

Rigorous Algorithms

- Conservative asynchronous algorithm

  Lubachevsky (1988), Korniss et al (1999), Shim & Amar (2004)

- Synchronous relaxation algorithm

  Lubachevsky & Weiss (2001), Shim & Amar (2004)

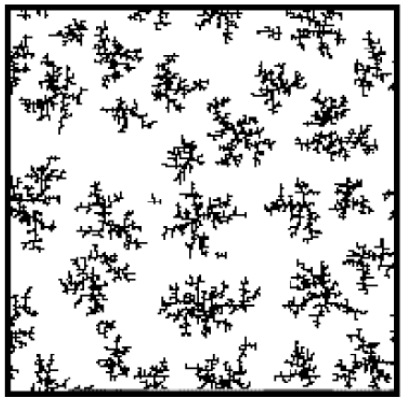

Thin film growth

Synchronous relaxation (SR) algorithm

(Lubachevsky & Weiss, 2001)

- All processors 'in-synch' at beginning & end of each cycle
- Iterative relaxation - at each iteration processors use boundary info. from previous iteration
- Relaxation complete when current iteration identical to previous iteration *for all processors*

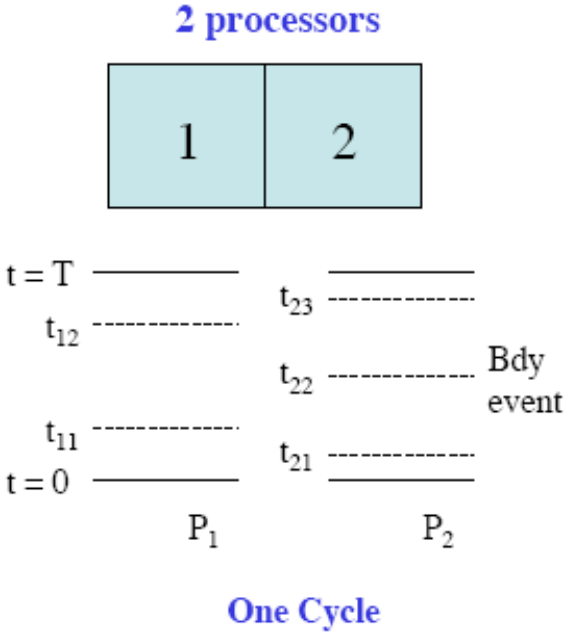

Parallel KMC

Disadvantages:

- ***Complex:*** requires 'keeping list' of all events, random numbers used in each iteration
- **Algorithm does not scale: faster** than CA algorithm but still **slow** due to *global synchronization* and requirement of *multiple iterations per cycle*

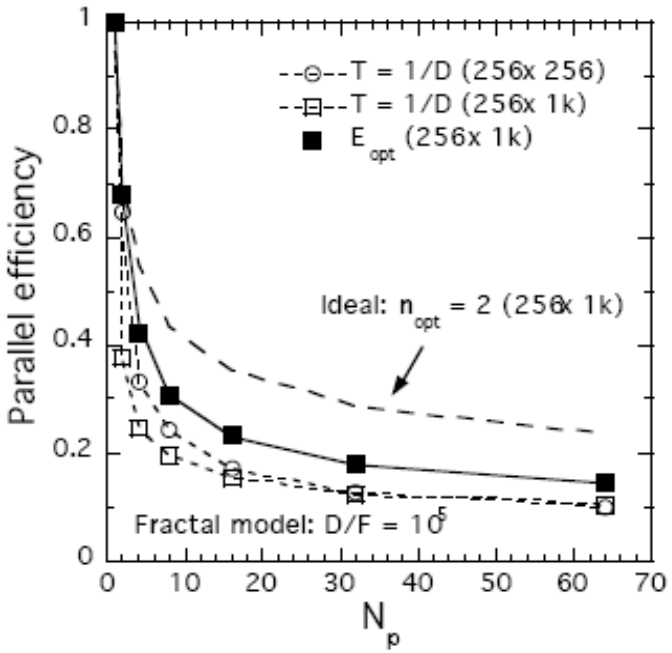

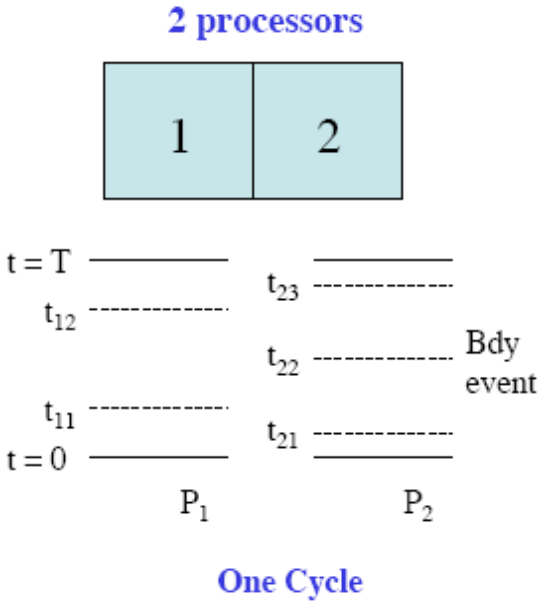

Hybrid KMC

Concurrent multi-scale models (See presentation by P. Geysermans)

Surface diffusion

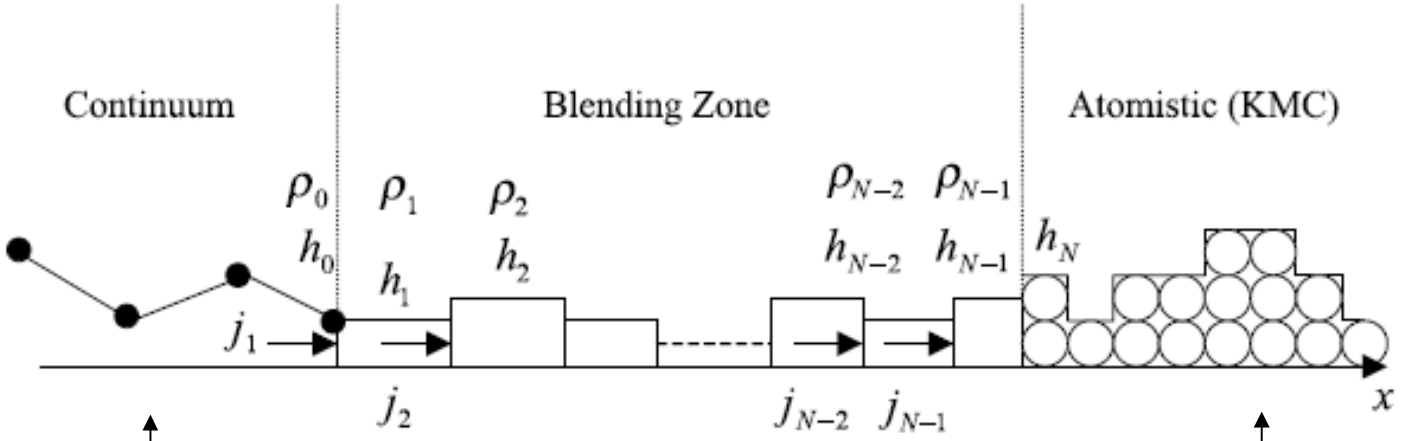

Gill, Spencer and Cocks, Materials Science and Engineering A365 (2004) 66–72

no (weak) crystal strain

Region of crystal strain

Self-learning KMC

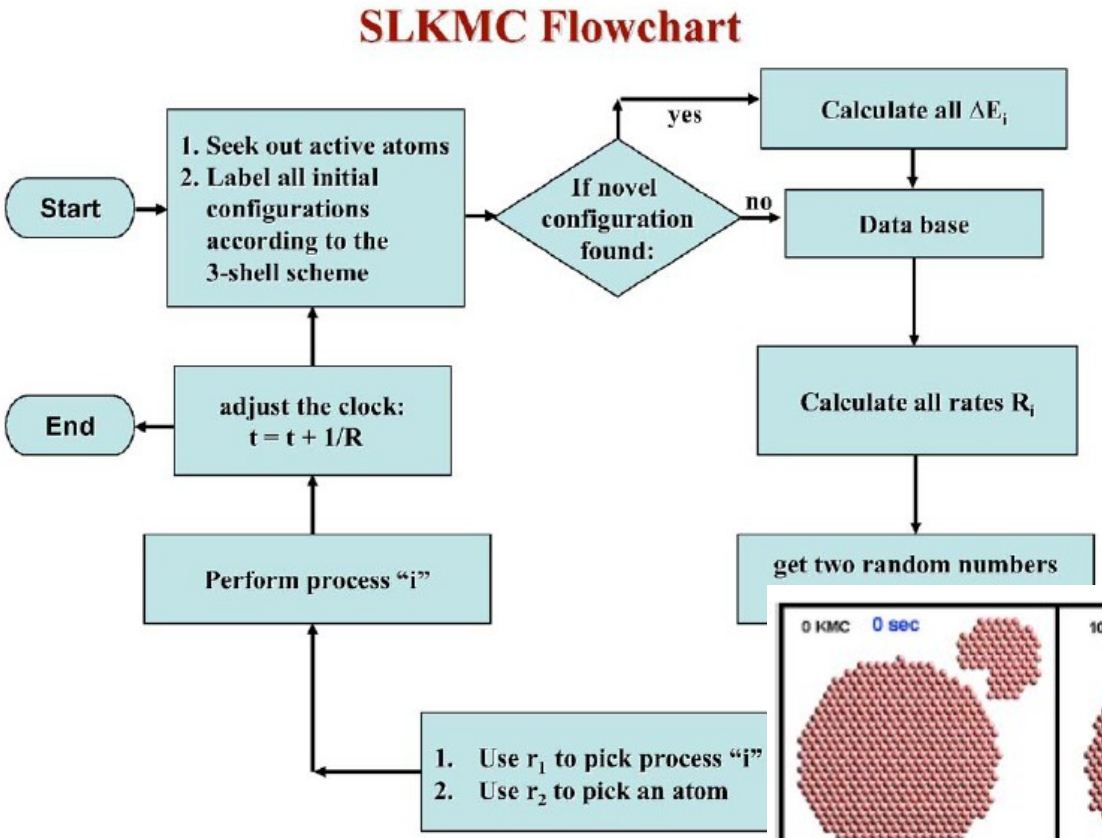

Trushin et al, PRB 72 (2005) 115401

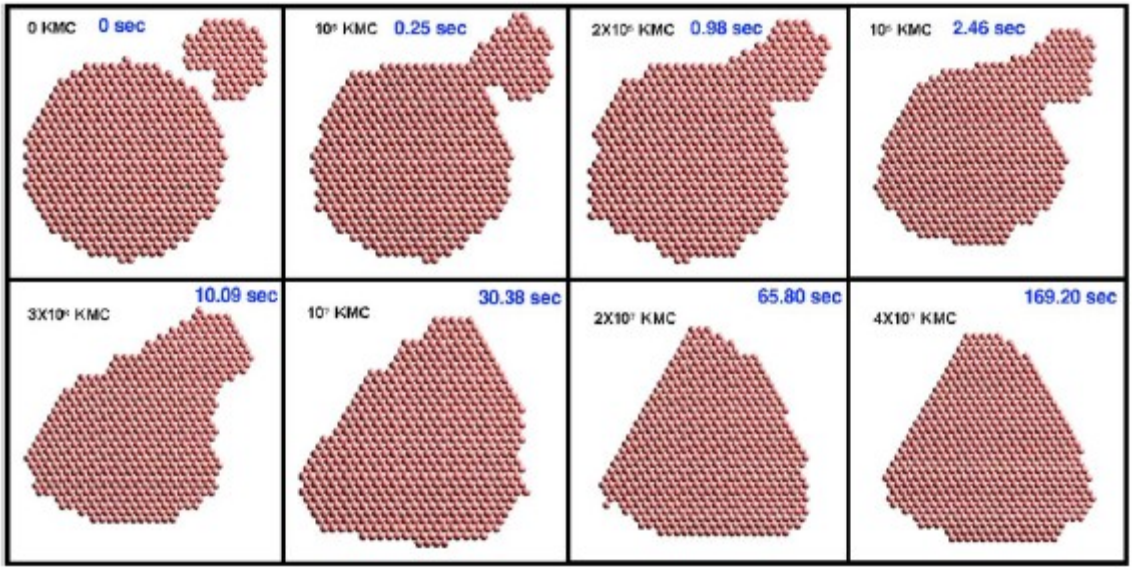

Outline

1. Introduction
   - Origin of Monte-Carlo methods
   - Time for Kinetic Monte-Carlo
2. Kinetic Monte-Carlo method
   - Physical motivation
   - Mathematical formalism
   - Numerical recipie
   - Range of applicability
   - Advanced methods
3. Applications
   - Atomistic KMC – thermal ageing & microstructure evolution
   - Object KMC – resistivity recovery

Atomistic KMC

- Rigid Lattice
- Atoms
- Vacancy (and interstitial) diffusion
- Recombination
- Binding energies

Atomistic KMC

Matrix + solute elements + vacancies + interstitials

Diffusion of vacancies and interstitials on a fixed lattice.

Vacancies: rigid lattice approximation, migrate to nearest neighbour.

Interstitials: migration depending on lattice type.

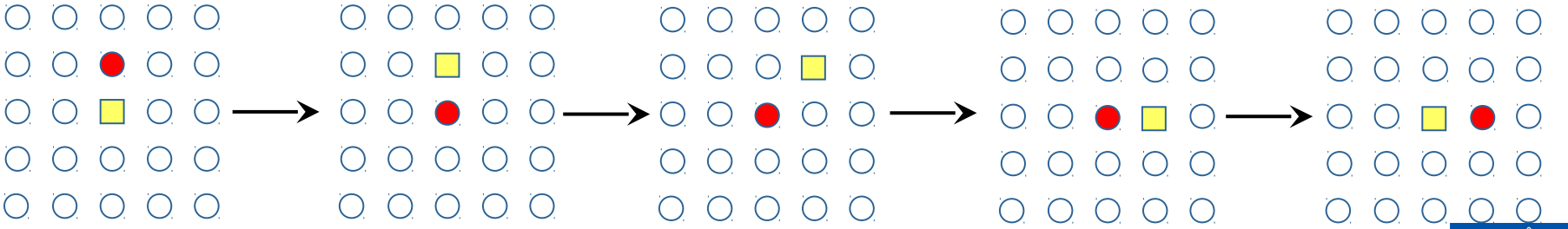

Atomistic KMC

- BCC metal: treatment of multi-component systems:
  - substitutional elements
  - vacancies
  - interstitials

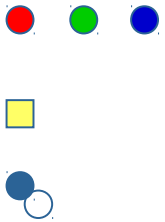

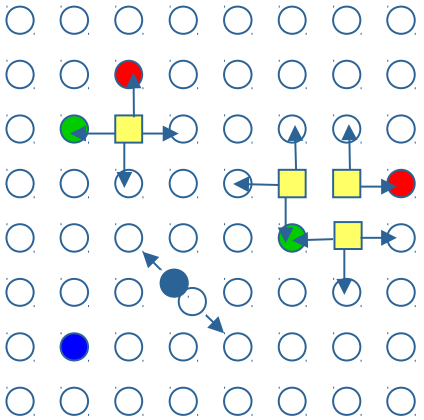

- Diffusion by first nearest neighbour jumps via:

vacancies

interstitials

Lattice diffusion:

$$D = D_0 \exp\left(-\frac{E_a}{kT}\right)$$

Jump frequency:

$$\Gamma = \nu \exp\left(-\frac{E_a}{kT}\right)$$

activation energy

attempt frequency

Atomistic KMC

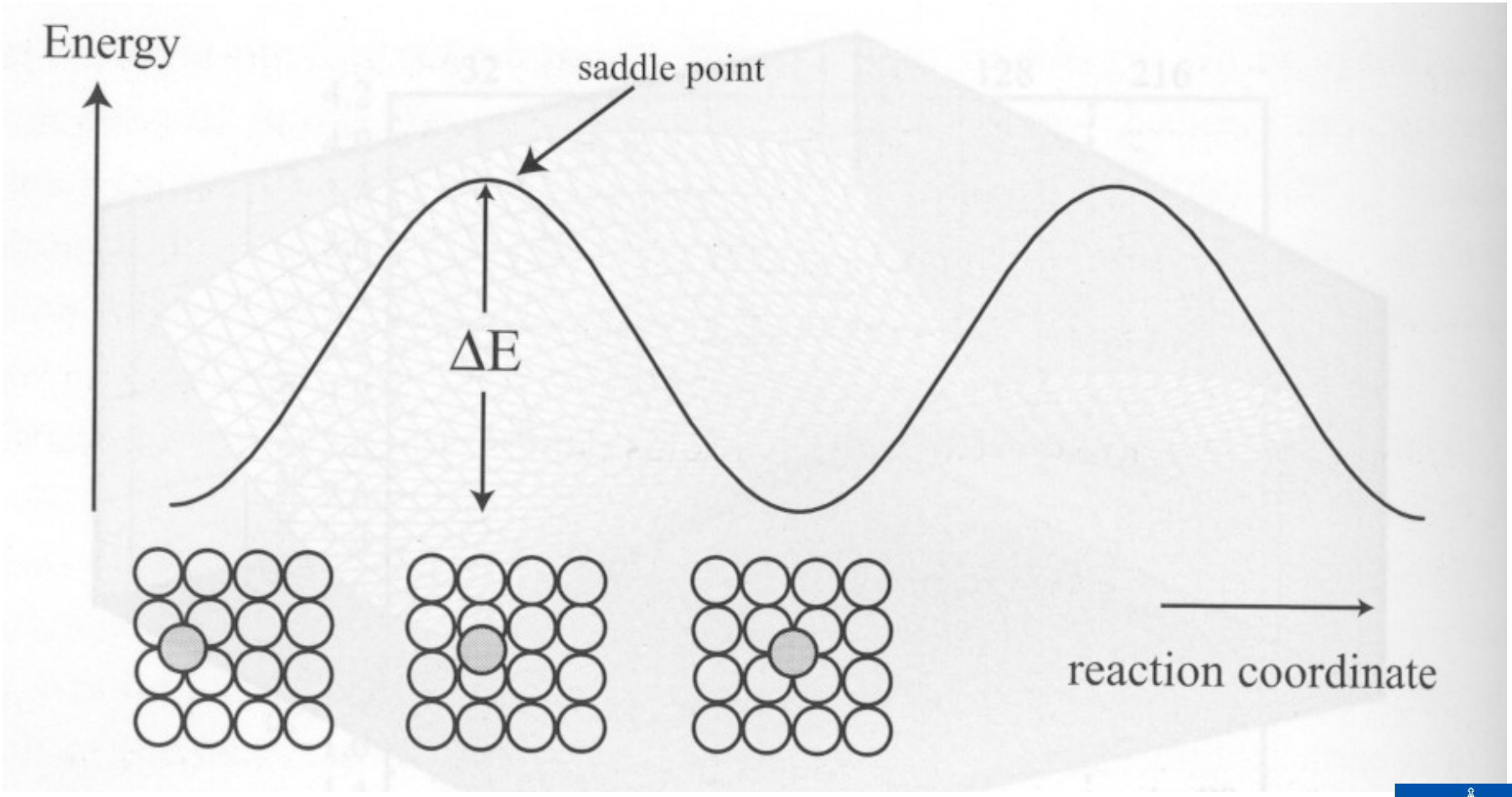

Atomistic KMC

How to get activation energy E_a?

Should obey detailed balance: $p_i r_{ij} = p_j r_{ji}$

a)

Direct migration energy calculation (MD or ab initio)

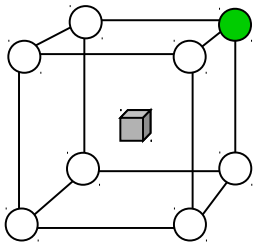

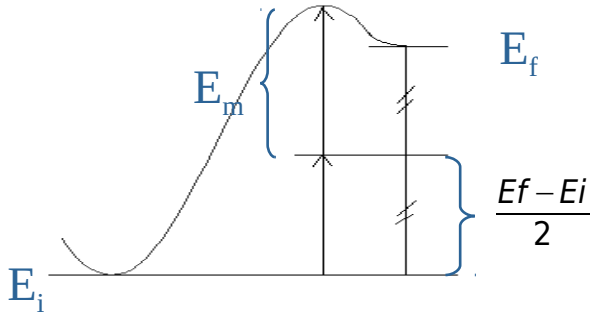

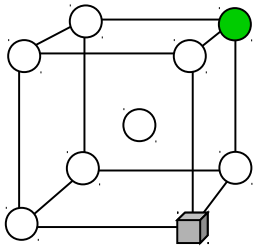

$$E_a = E_m + \frac{E_f - E_i}{2}$$

Atomistic KMC

b)

Jump frequency of point defects

$$\Gamma_A = \nu_A \exp\left\{-\frac{\Delta E_A^{act}}{k_b T}\right\}$$

attempt frequency — migration barrier

ΔE_a = E(sad) - E(ini)

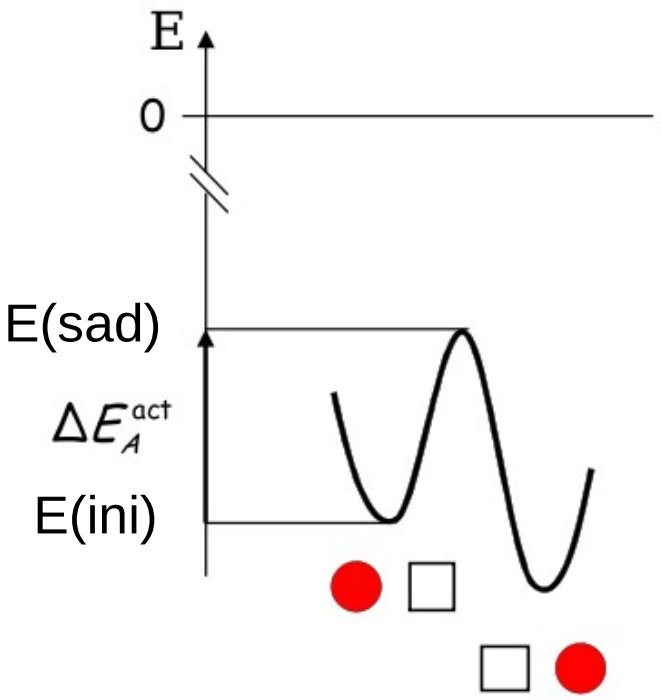

F. Soisson, A. Barbu and G. Martin, Acta Mater. 44 (1996) 3789.

Atomistic KMC

b)

Jump frequency of point defects

$$\Gamma_A = \nu_A \exp\left\{-\frac{\Delta E_A^{act}}{k_b T}\right\}$$

attempt frequency — migration barrier

$$\Delta E_A^{act} = E(sad) - E(ini) = e_A^{sad} - \Sigma V_{Aj} - \Sigma V_{iV}$$

bond energy for A at saddle

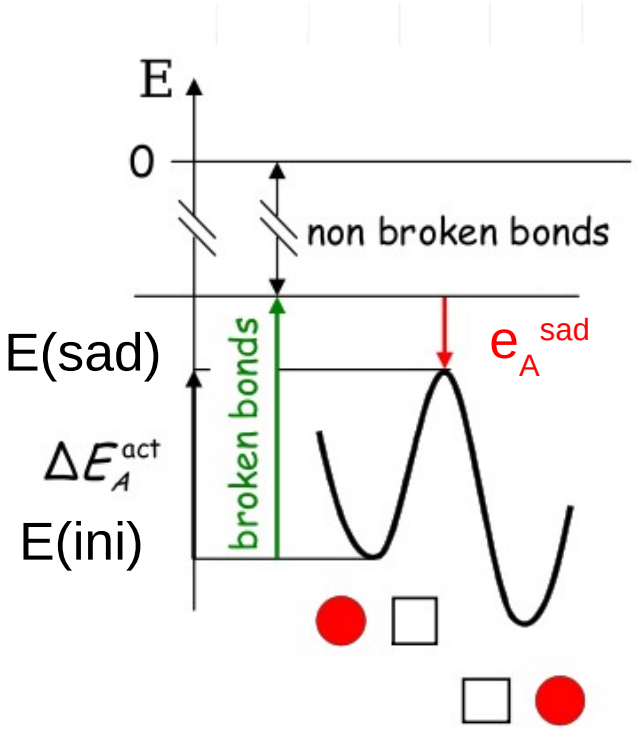

F. Soisson, A. Barbu and G. Martin, Acta Mater. 44 (1996) 3789.

Atomistic KMC

- BCC metal: treatment of multi-component systems:
  - substitutional elements
  - vacancies
  - interstitials

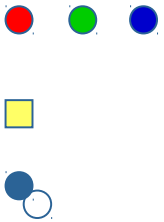

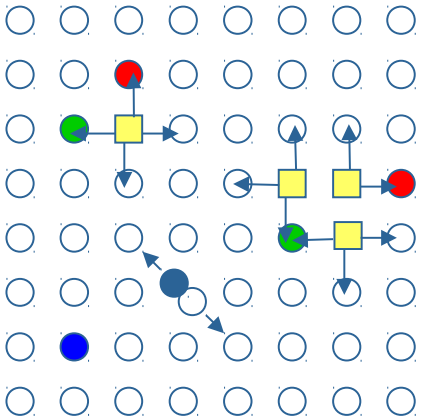

- Diffusion by first nearest neighbour jumps via: vacancies
  interstitials

Jump probability $\Gamma_x = \nu_x e^{-\frac{E_a}{kT}}$ ν_X is the attempt frequency

- Residence time algorithm

Applied to vacancy and interstitial jumps

Average time step: $\Delta t = \frac{1}{\sum_{j,k} \Gamma_{jk}}$

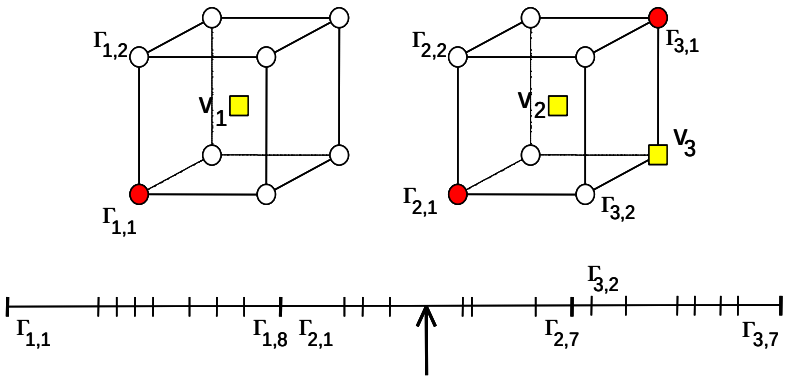

Thermal ageing of Fe-Cr alloys

Fe-Cr alloys are very interesting for nuclear applications:

- Swelling resistance
- Low ductile-brittle transition temperature
- Creep resistance
- Corrosion resistance
- etc.

Olsson, Abrikosov, Wallenius

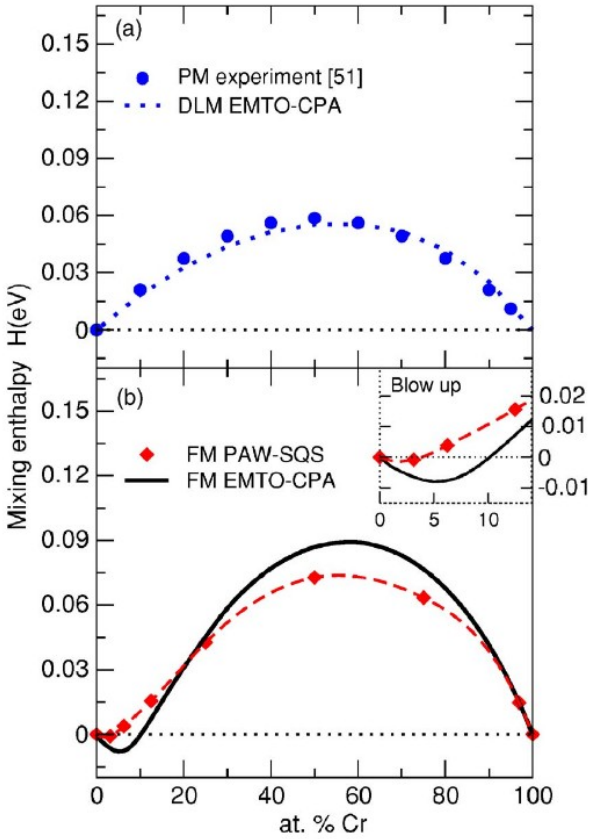

Terentyev, PhD thesis, SCK-CEN

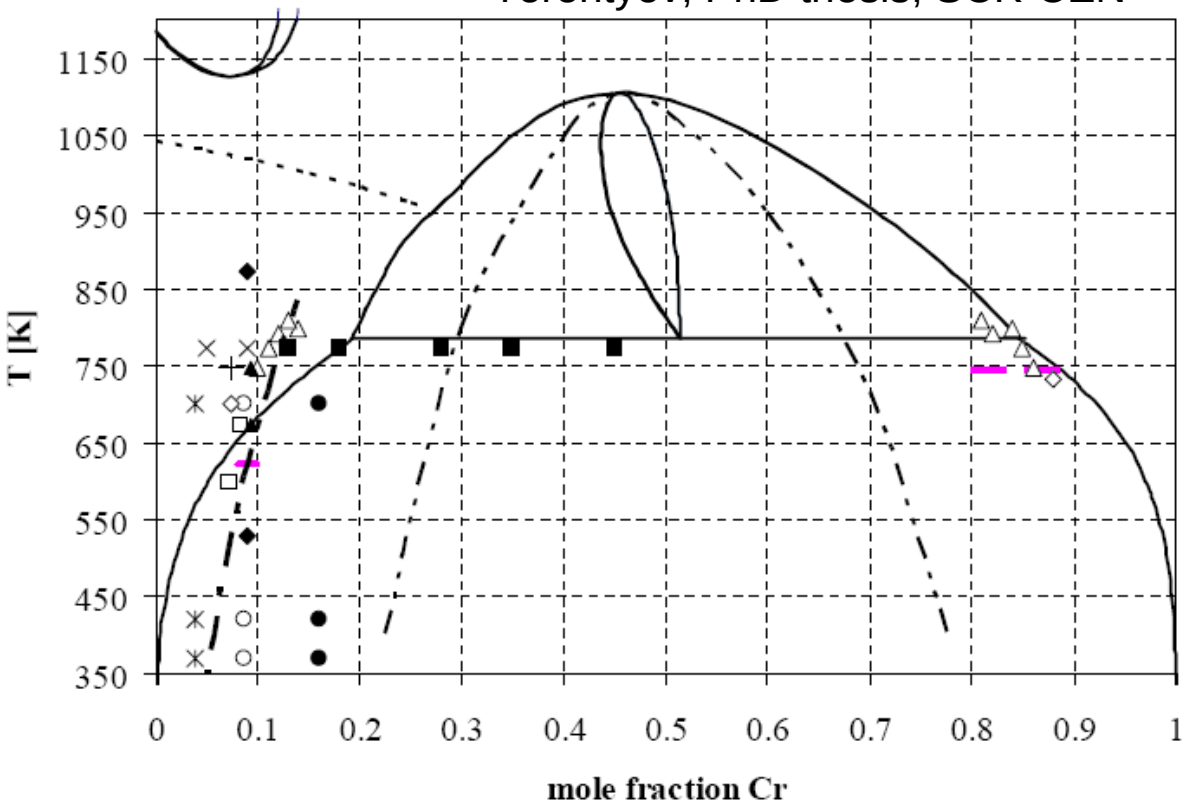

Thermal ageing of Fe-Cr alloys

Tomographic Atom Probe (TAP) at Univ. Rouen: ageing study on model Fe-Cr alloys and real steels

$$Dd_{Cr} = d_{Cr\text{-}Cr} - d_{X\text{-}Y}$$

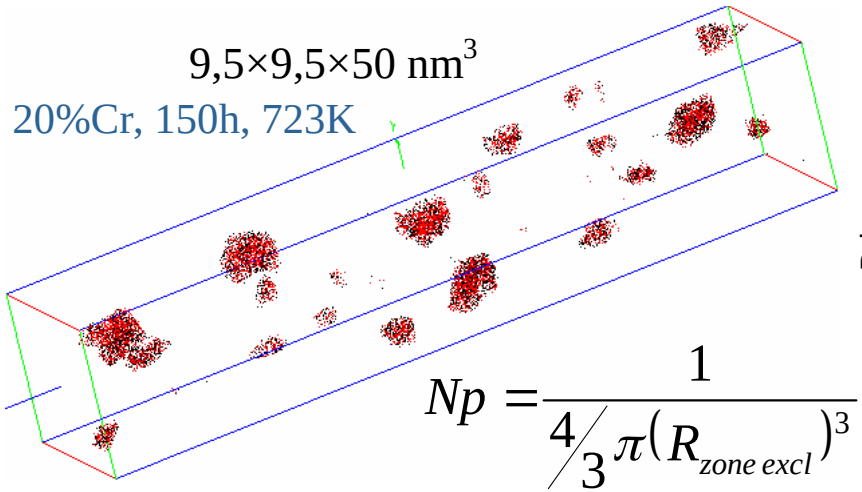

$$Np = \frac{1}{\frac{4}{3}\pi (R_{zone\ excl})^3}$$

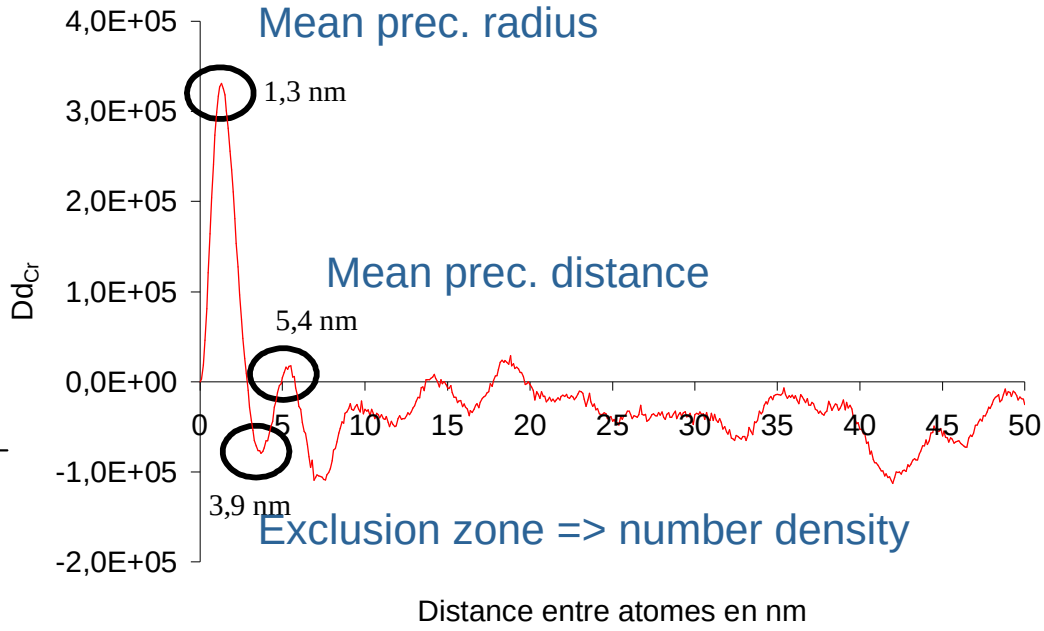

Thermal ageing of Fe-Cr alloys

Vacancy driven atomistic KMC:

only process is the single vacancy jump

only one vacancy (still supersaturated simulation cell)

cohesion model: concentration dependent interatomic potential.

Olsson et al PRB 72 (2005)

Residence time algorithm:

$$\Gamma_x = \nu_x e^{-\frac{E_a}{kT}}$$

$$E_a = E_m + \frac{E_f - E_i}{2}$$

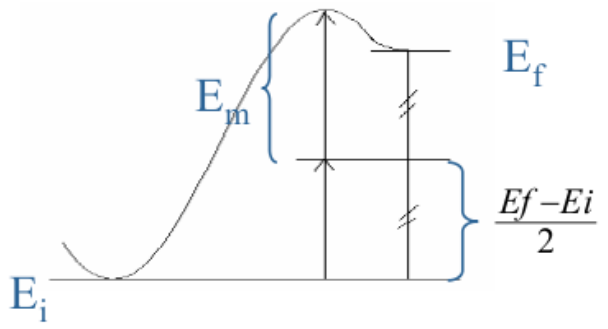

Average time step: $\Delta t = \frac{1}{\sum_i \Gamma_i}$

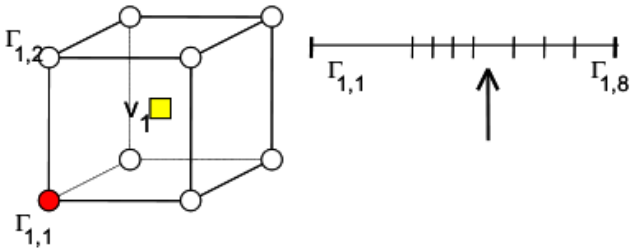

Thermal ageing of Fe-Cr alloys

Short range order

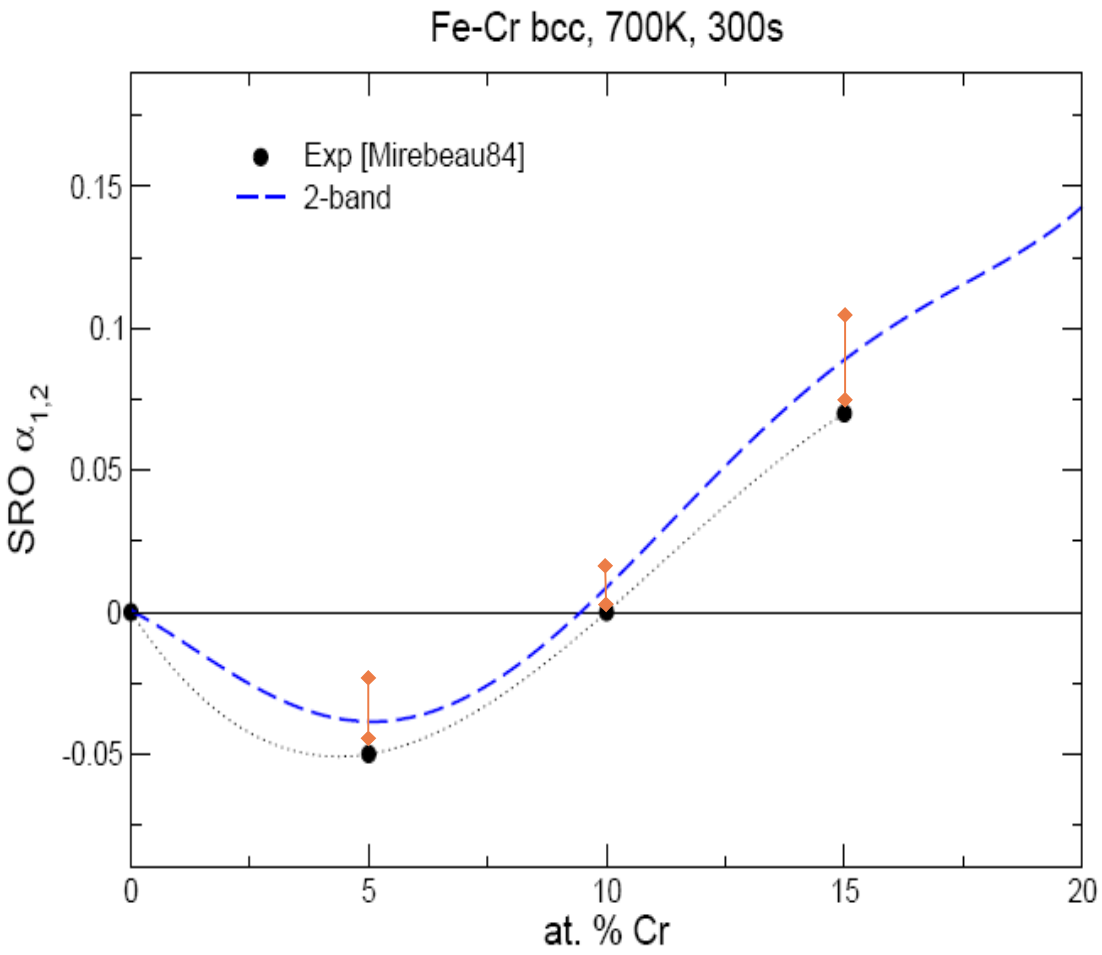

Due to supersaturation of vacancies, the simulated KMC time is not directly comparable to real time.

"Real" time from KMC time scaled to equilibrium vacancy concentration:

$$C_{\mathrm{vac}}^{\mathrm{eq}} = \exp\left(-\frac{G_{\mathrm{f}}}{kT}\right)$$

$$\Delta t = C_{\mathrm{vac}}^{\mathrm{eq}} \Delta t_{\mathrm{KMC}}$$

Thermal ageing of Fe-Cr alloys

Fe-10Cr after 1 week

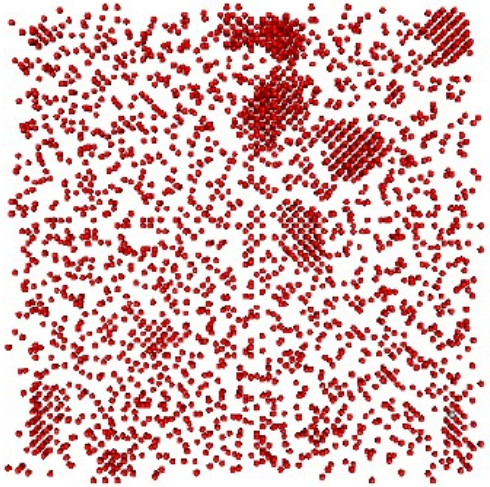

743K

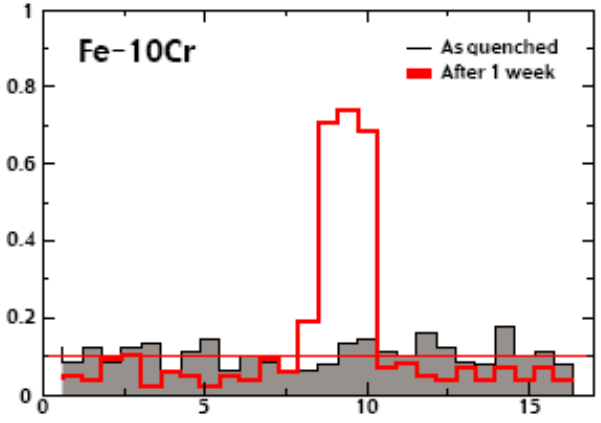

Fe-32Cr after 1 month

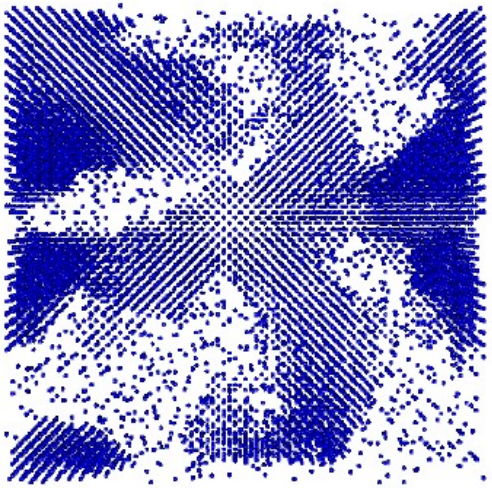

743K

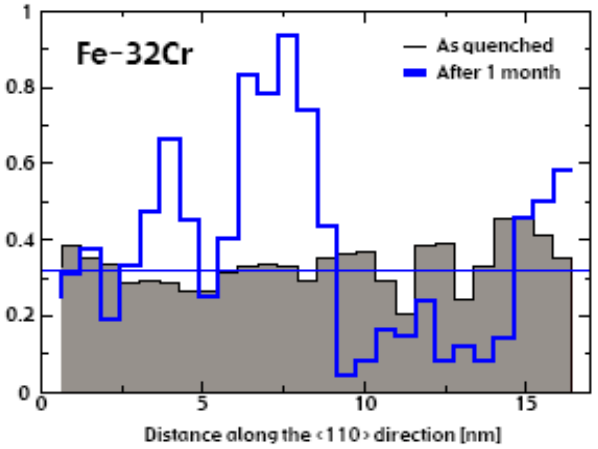

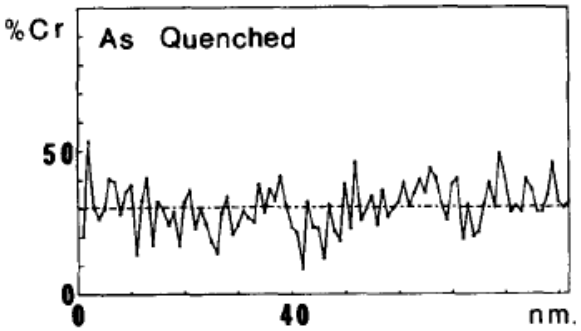

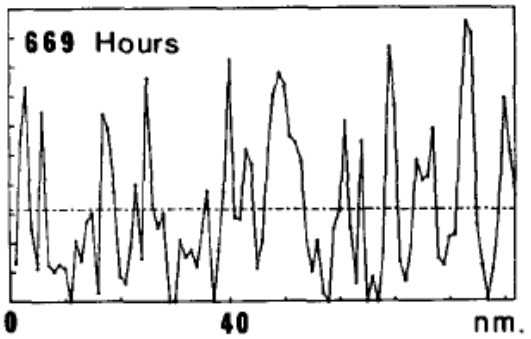

Fe-32Cr, 743K, 669h

Brenner -82

Homogeneous precipitation in bulk Fe-Cr

T = 750K ; x_{Cr} = 0.15

Cr precipitates when fluctuations become larger than a critical size

Precipitates are spherical

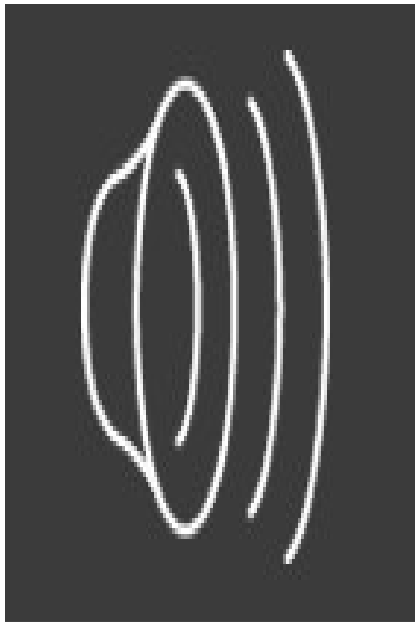

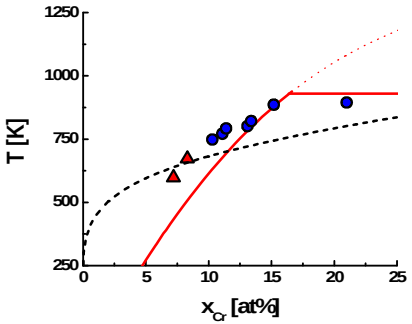

Courtesy: A. Caro

Spinodal decomposition in bulk Fe-Cr

Homogeneous precipitation at x_{Cr}~0.5, within the spinodal

Spinodal decomposition happens by growth of small composition fluctuations

(diffusion against the gradient of x),

in regions of the phase diagram where $d^2G/dx^2 < 0$

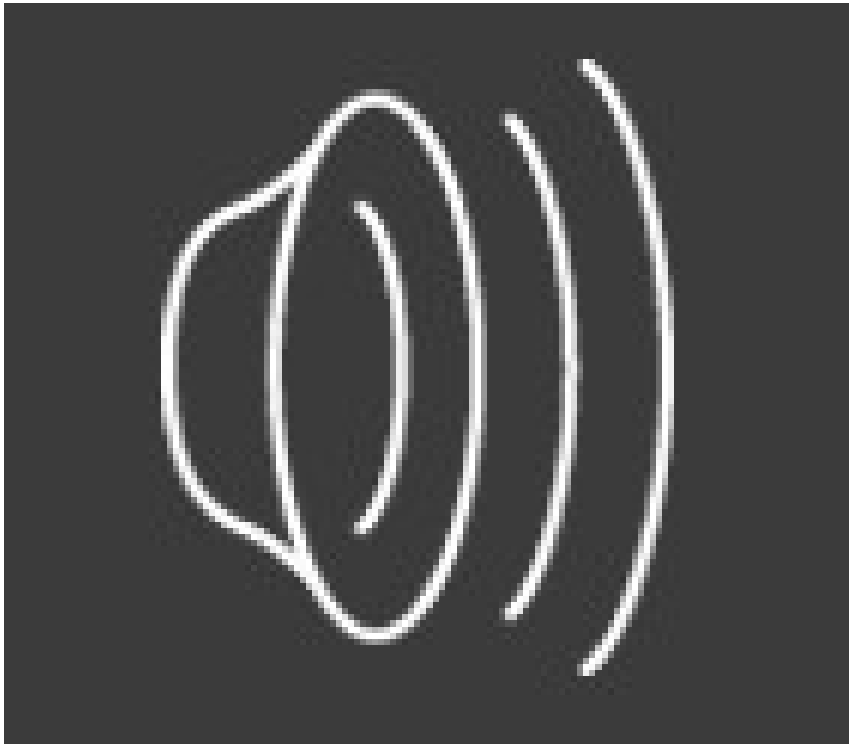

Cr precipitation in $Fe._5Cr._5$ at 750K

2-D slice of a 3D sample

Microstructural evolution in RPV steels

RPV steels:
Matrix Fe
+ alloying elements: Cu, Ni, Mn, Si, …
+ carbon, nitrogen
+ dislocations

0,08 dpa – Neutron irradiation

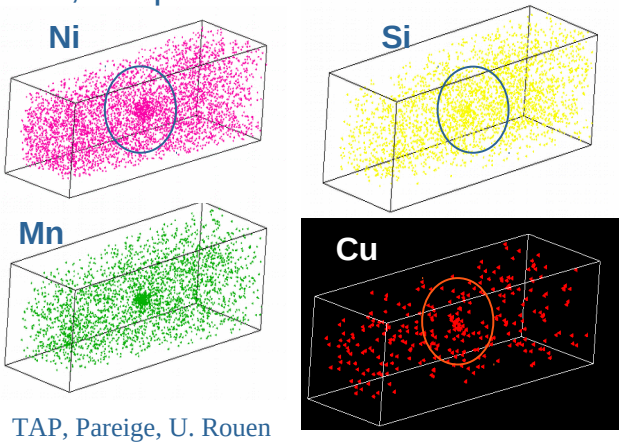

TAP, Pareige, U. Rouen

15x15x50 nm

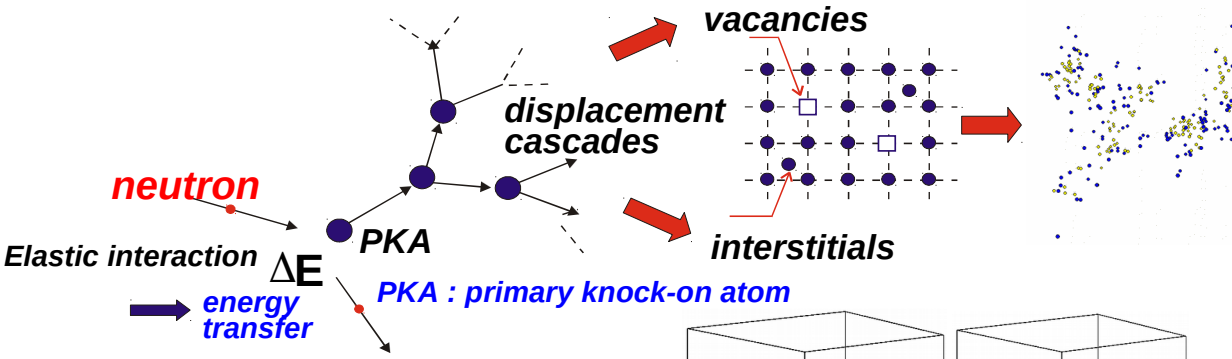

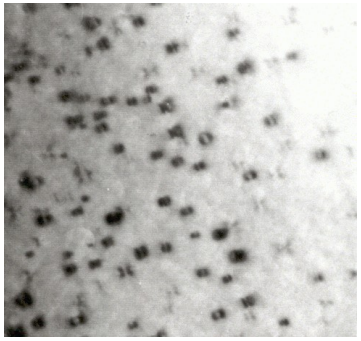

TEM, Barbu, CEA

Microstructure evolution:
point defect clusters: nanovoids,
dislocation loops
solute clusters (w or w/o point defects)

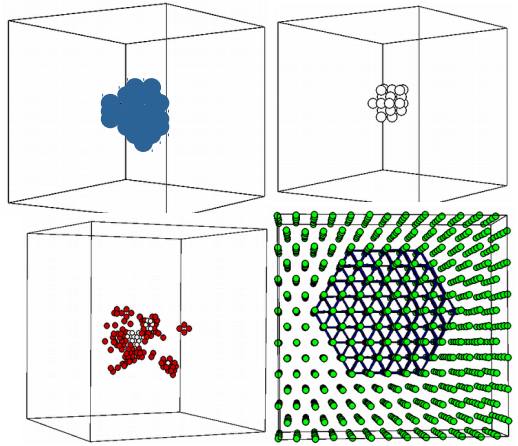

Microstructural evolution in RPV steels

- Multi-component system treated by Atomistic KMC:
  - substitutional elements (Cu, Ni, Mn, Si)
  - interstitials (Fe, Cu, Ni, Mn, Si)

  Cohesive model by interatomic potential not feasible!

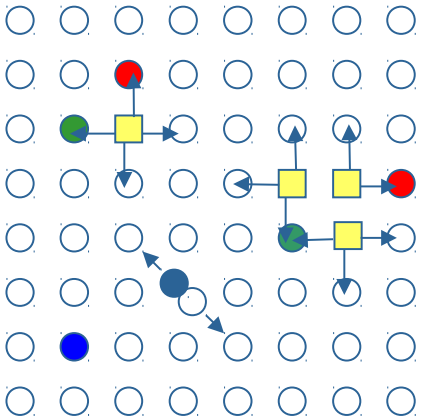

- Diffusion by first nearest jumps via vacancies
  interstitials

Jump probability $\Gamma_X = \nu_X \exp\left(-\frac{Ea}{kT}\right)$ ν_X attempt frequency

- Residence time algorithm

Applied to vacancy and interstitial jumps

Average time step: $\Delta t = \frac{1}{\sum_{j,k} \Gamma_{jk}}$

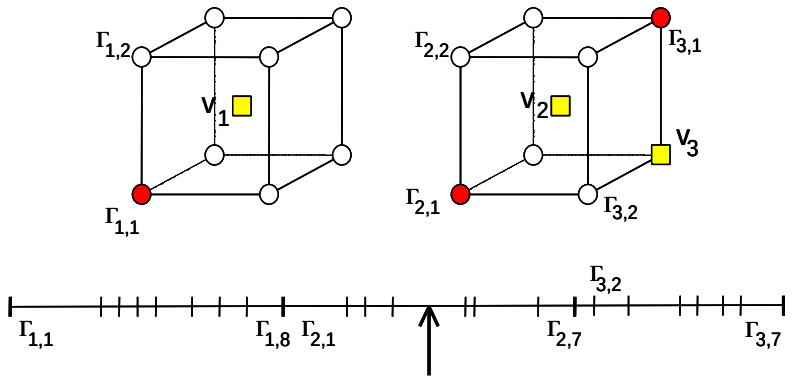

Microstructural evolution in RPV steels

Environment dependent form for the activation energy

$$Ea = Ea_0 + \frac{Ef - Ei}{2}$$

Ea_0 = ab initio migration energy via a vacancy of the migrating atom in an α-Fe matrix

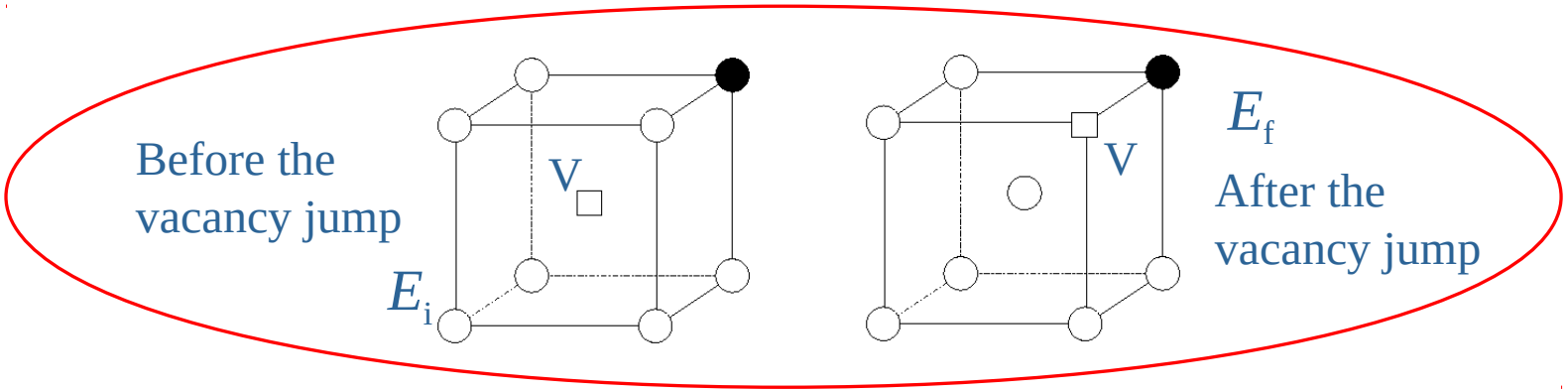

DFT data	Fe	Cu	Ni	Mn	Si
$E_{migration}$ (X) (eV)	0.62	0.54	0.68	1.03	0.42

Microstructural evolution in RPV steels

Cohesive model based on pair interactions up to second nearest neighbours

$$Ea = Ea_0 + \frac{Ef - Ei}{2}$$

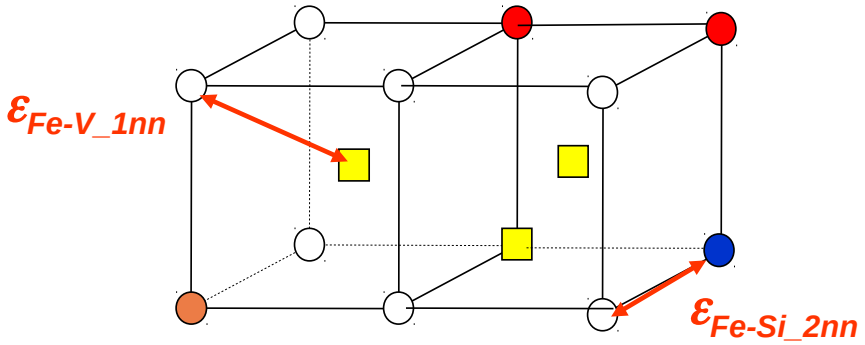

$$E = \sum_j \varepsilon^{(i)}_{(Fe\text{-}Fe)} + \sum_k \varepsilon^{(i)}_{(V\text{-}V)} + \sum_l \varepsilon^{(i)}_{(Fe\text{-}V)} + \sum_m \varepsilon^{(i)}_{(Fe\text{-}X)} + \sum_n \varepsilon^{(i)}_{(V\text{-}X)} + \sum_p \varepsilon^{(i)}_{(X\text{-}Y)}$$

i = 1 or 2, corresponds to first or second nearest neighbour interaction

j = the number of Fe-Fe bonds

k = the number of V-V bonds

l = the number of Fe-V bonds

m = the number of Fe-X bonds

n = the number of V-X bonds

p = the number of X-Y bonds

X, Y = solute atoms (Cu, Ni, Mn or Si)

Microstructural evolution in RPV steels

Binary alloys

$$E_{mixing} = -4\varepsilon^{(1)}_{(Fe\text{-}Fe)} - 3\varepsilon^{(2)}_{(Fe\text{-}Fe)} + 8\varepsilon^{(1)}_{(Fe\text{-}X)} + 6\varepsilon^{(2)}_{(Fe\text{-}X)} - 4\varepsilon^{(1)}_{(X\text{-}X)} - 3\varepsilon^{(2)}_{(X\text{-}X)}$$

$$E_{interface(100)} = -2\varepsilon^{(1)}_{(Fe\text{-}Fe)} - \varepsilon^{(2)}_{(Fe\text{-}Fe)} + 4\varepsilon^{(1)}_{(Fe\text{-}X)} + 2\varepsilon^{(2)}_{(Fe\text{-}X)} - 2\varepsilon^{(1)}_{(X\text{-}X)} - \varepsilon^{(2)}_{(X\text{-}X)}$$

$$E_{coh}(Z) = 4\varepsilon^{(1)}_{(Z\text{-}Z)} + 3\varepsilon^{(2)}_{(Z\text{-}Z)}$$

$$E_{formation}(V^Z) = 8\varepsilon^{(1)}_{(V\text{-}Z)} + 6\varepsilon^{(2)}_{(V\text{-}Z)} - 4\varepsilon^{(1)}_{(Z\text{-}Z)} - 3\varepsilon^{(2)}_{(Z\text{-}Z)}$$

$$E^{(i)}_{binding(V\text{-}V)} = 2\varepsilon^{(i)}_{(Fe\text{-}V)} - \varepsilon^{(i)}_{(Fe\text{-}Fe)} - \varepsilon^{(i)}_{(V\text{-}V)}$$

$$E^{(1)}_{binding(V\text{-}X)} = \varepsilon^{(1)}_{(Fe\text{-}V)} + \varepsilon^{(1)}_{(Fe\text{-}X)} - \varepsilon^{(1)}_{(Fe\text{-}Fe)} - \varepsilon^{(1)}_{(V\text{-}X)}$$

Z = Fe or solute atom

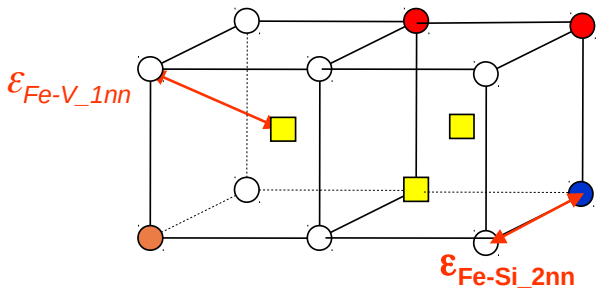

Ternary alloys

$$E^{(i)}_{binding(X\text{-}Y)} = \varepsilon^{(i)}_{(Fe\text{-}X)} + \varepsilon^{(i)}_{(Fe\text{-}Y)} - \varepsilon^{(i)}_{(Fe\text{-}Fe)} - \varepsilon^{(i)}_{(X\text{-}Y)}$$

i = 1 or 2

X, Y = solute atoms

Ab initio data **Parameters**

Microstructural evolution in RPV steels

VASP, SGGA, USPP, constant volume relaxation, cut off : 240 eV, 54 or 128 atoms with 125 or 27 k points

Point defect-solute binding energies

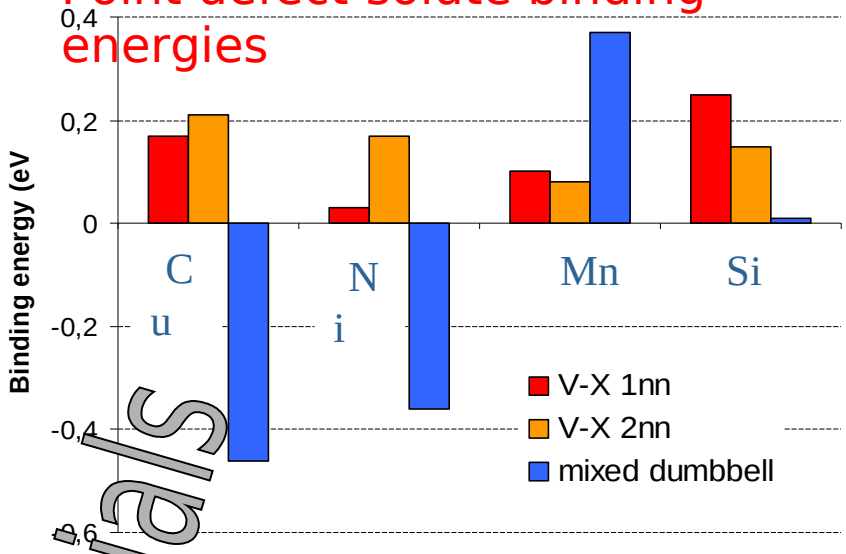

Solute Migration energies

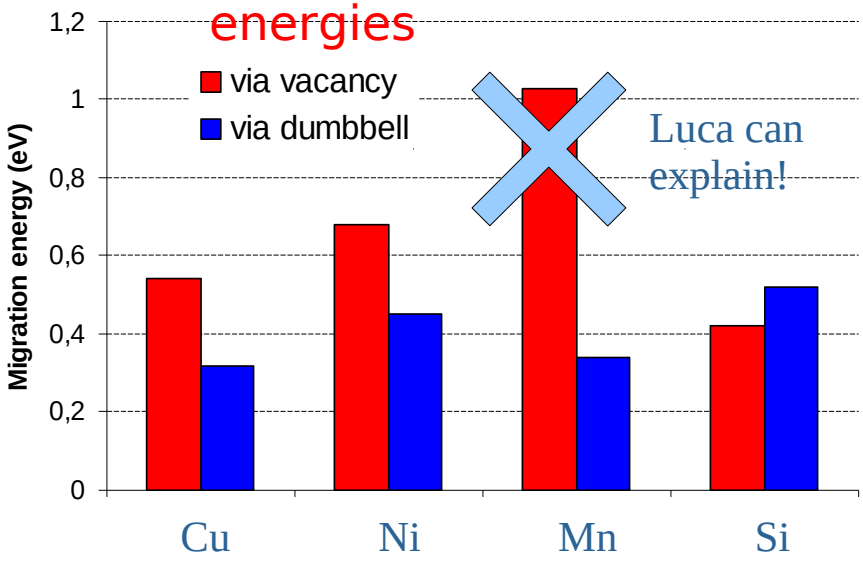

Interstitials

Mn

- high mixed dumbbell binding energy
- low migration energy via dumbbells

Contrary to the other solutes,
Mn may diffuse preferentially via an interstitial mechanism

KTH VETENSKAP OCH KONST

Microstructural evolution i

- Solute-dumbbell binding energy

dumbbell atoms
Solute atoms
Fe atoms

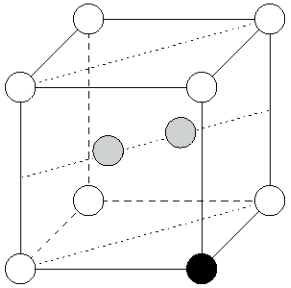

1nn^{Tens}_‹110›

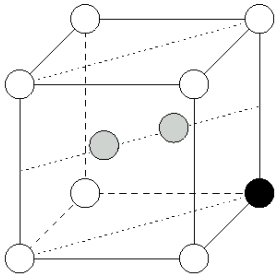

1nn^{Comp}_‹110›

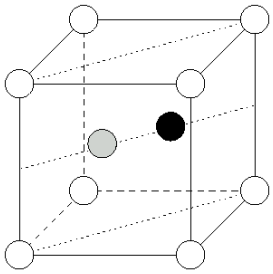

‹110›_mixed

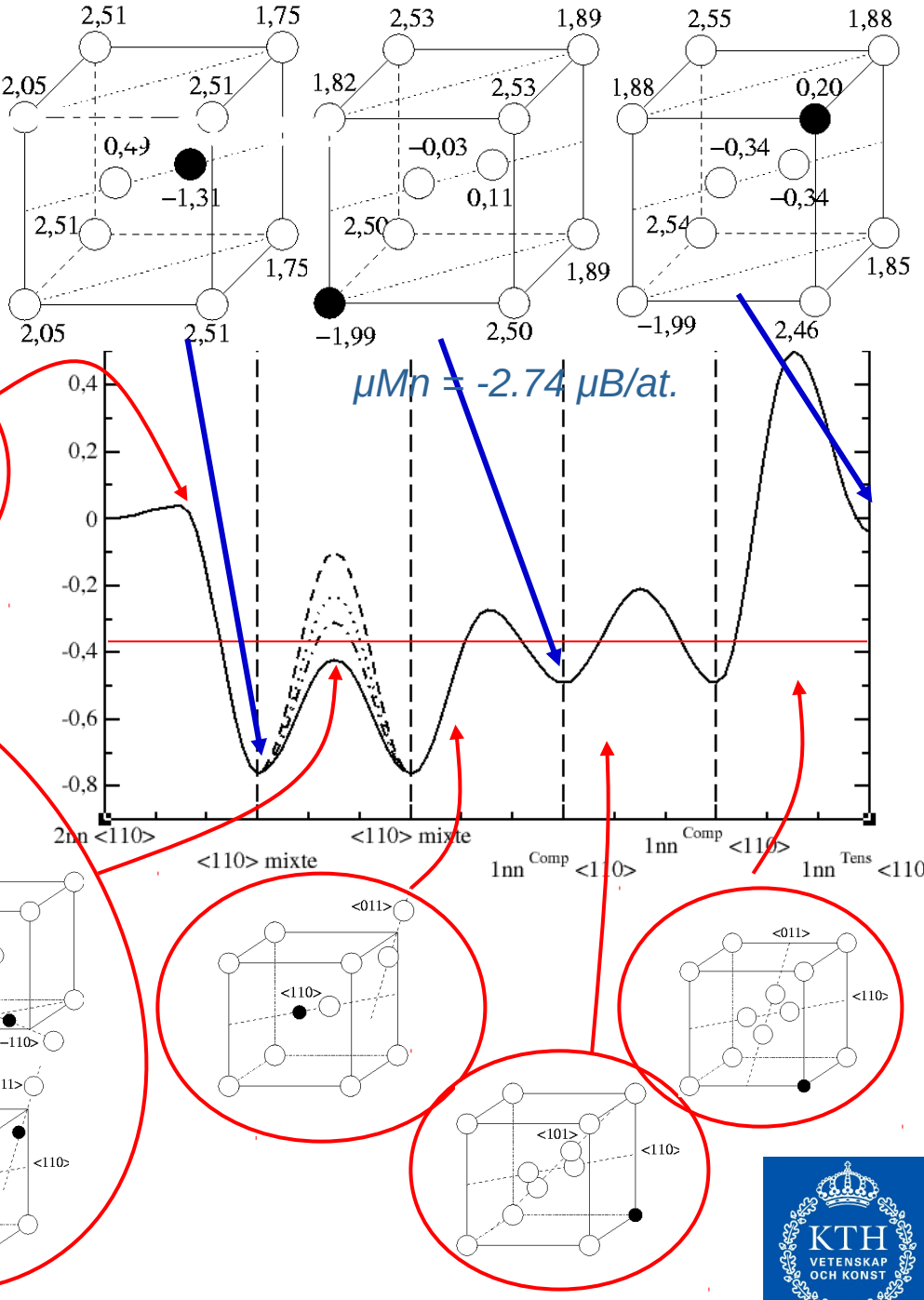

Microstructural evolution in RPV steels

Environment dependent form for the activation energy

$$Ea = Ea_0 + \frac{Ef - Ei}{2}$$

Ea_0 = ab initio migration-60° rotation energy of the migrating atom in an α-Fe matrix

Ei

Before the interstitial jump

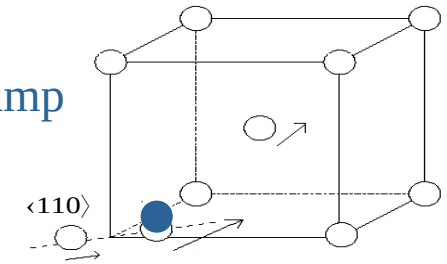

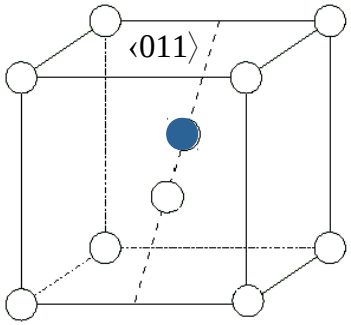

Ef

After the interstitial jump

	Fe-Fe dumbbell	Fe-Cu dumbbell	Fe-Ni dumbbell	Fe-Mn dumbbell	Fe-Si dumbbell
Migration energy (eV)	**0.37**	**0.32**	**0.45**	**0.34**	**0.52**

Microstructural evolution in RPV steels

Direct calculation

Complex binding energies

(1 dumbbell + several solute atoms)

⟺

Indirect calculation

Sum of elementary binding energies of the complex

$$Ea = Ea_0 + \frac{Ef - Ei}{2}$$

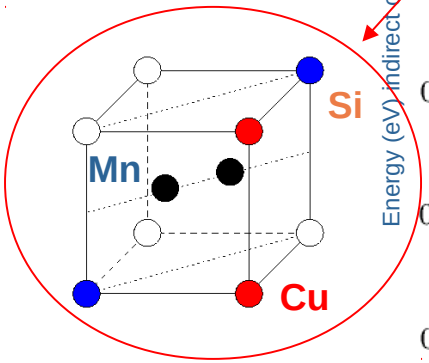

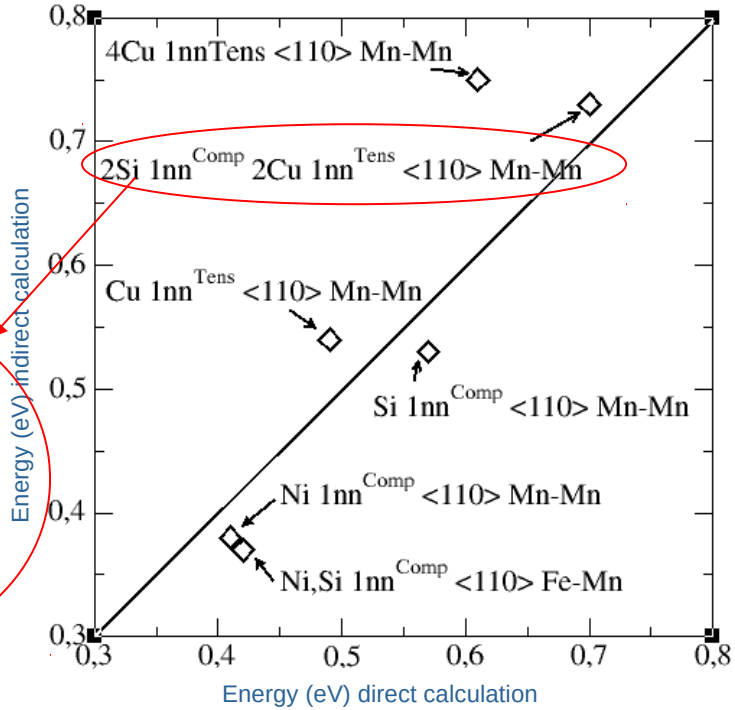

Complex binding energy addition:

- solute - dumbbell

Solute atoms

Fe atom

$E_l^{mixed}(X_j - X_k)$

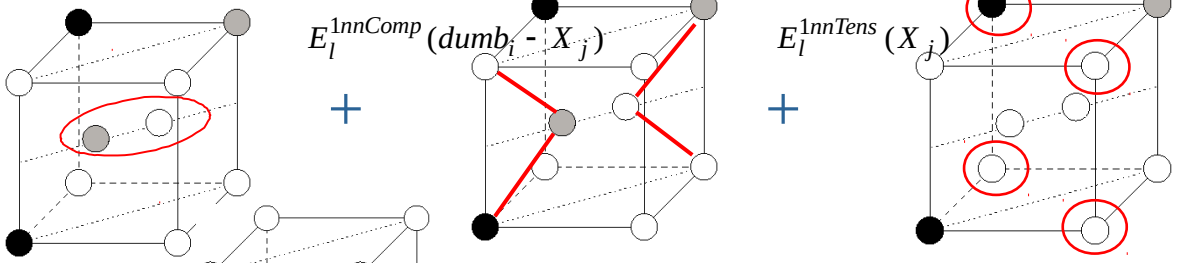

- dumbbell - dumbbell

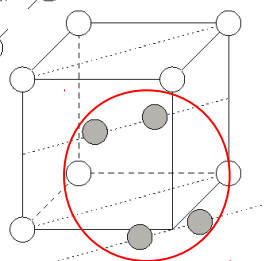

$E_l(dumb - dumb)$

Microstructural evolution in RPV steels

"NEUTRON" IRRADIATION of FeCuNiMnSi ALLOY

Fe-0.2Cu-0.53Ni-1.26Mn-0.63Si (%at.) at 300°C

Flux: 6.5 10^{-4} dpa.s^{-1}, Dose: 2 10^{-3} dpa

For neutron irradiation:
- flux of 20 keV and 100 keV cascades debris obtained by Molecular Dynamics
(R. Stoller, J. Nucl. Mater. 307-311 (2002) 935)

+

Frenkel pairs

(For electron irradiation: Frenkel pair flux)

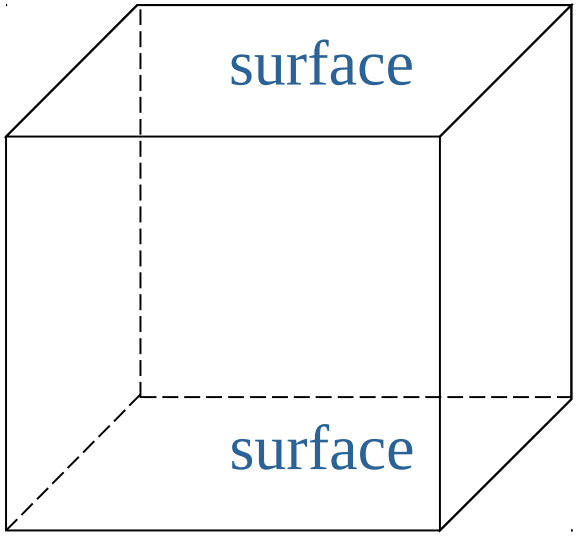

Surfaces along z direction

$100a_0 \times 100a_0 \times 100a_0$

$\sim(30\ nm)^3$

Cu Mn la
Ni Si c SIA

Cu
Si
Mn
Ni
V
SIA

Ni effect under electron irradiation

Flux: 5.10^{-8} dpa.s^{-1} ; dose: 1-1.2.10^{-3} dpa ; T: 300 °C

Ni effect:

- Similar cluster density
- No modifications of Cu precipitation

Good agreement with exp. results

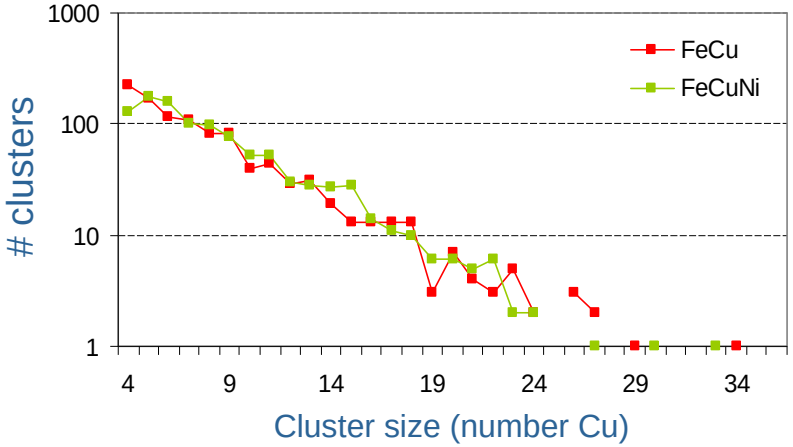

(F. Maury et al., J. Nucl. Mater. 183 (1991) 217 ; M.H. Mathon, PhD (1994))

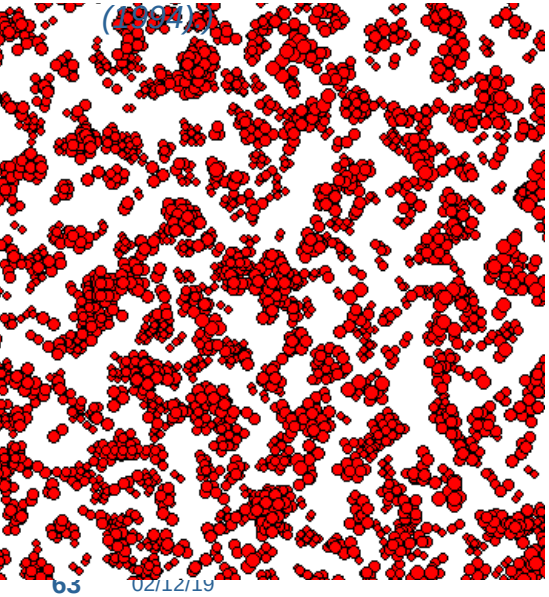

Fe-1.34 %at. Cu

Fe-1.4 %at. Cu-1.4 %at. Ni

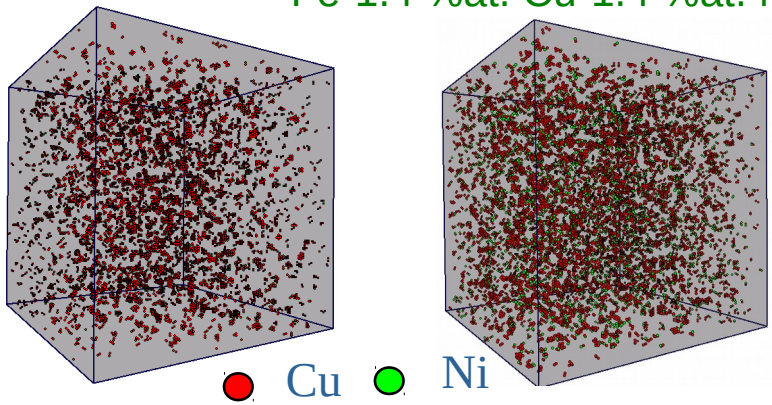

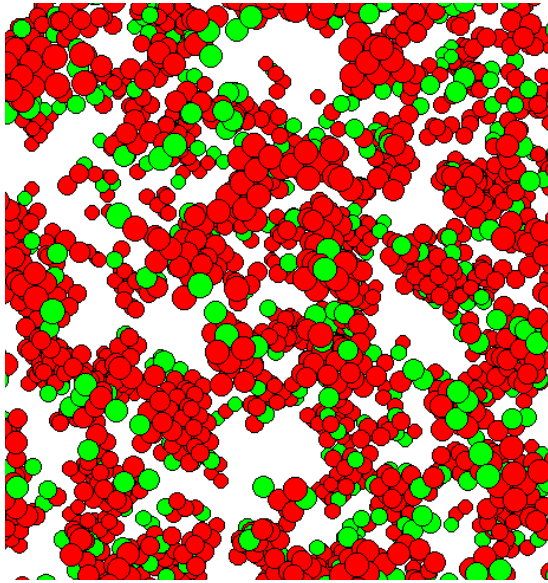

$100a_0 \times 100a_0 \times 100a_0$ *Surfaces along z axis*

Flux effect under neutron irradiation

Fe-0.79 %at. Cu at 300°C **Dose: 5 10^{-4} dpa**

Bigger Cu and vacancy-solute complex clusters with the lower flux

Good agreement with exp. results

(S. Yanagita et al., ASTM STP 1366 (2000) 516; R. Kasada et al., ASTM STP 1405 (2001) 237.)

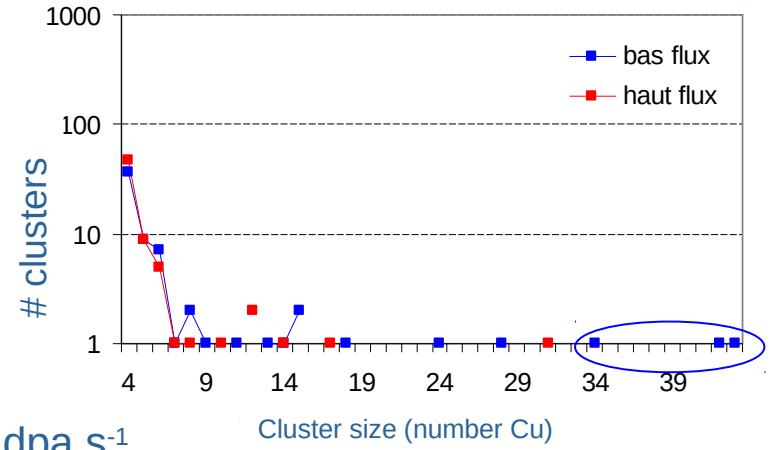

High flux: 2 10^{-5} dpa.s^{-1}

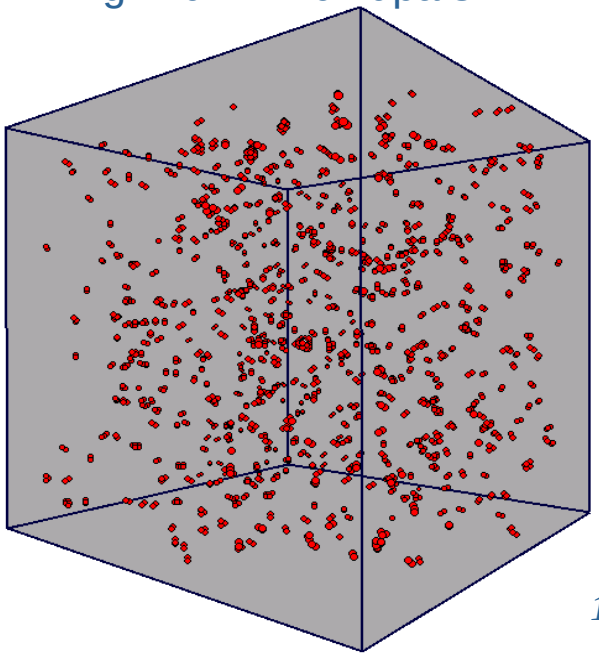

Cu

vac

SIA

Surfaces along z direction

$100a_0 \times 100a_0 \times 100a_0$

"Low" flux: 7 10^{-6} dpa.s^{-1}

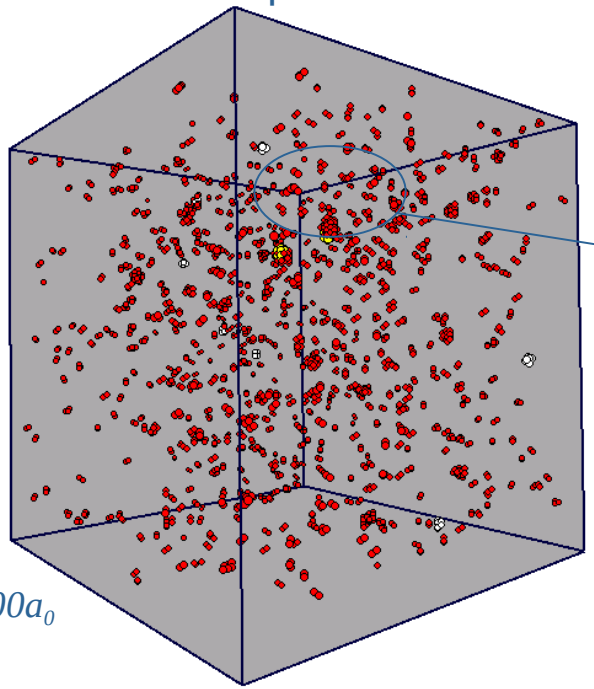

11 vac + 43 Cu

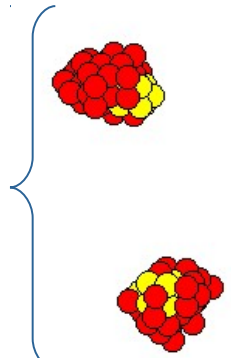

11 vac + 42 Cu

Mn effect under neutron irradiation

Flux: 0.5-1.0 10^{-5} dpa.s^{-1} Dose: 1.6-1.7 10^{-3} dpa

Mn effect:

- higher cluster density, seemingly smaller clusters
- no vacancy-solute clusters

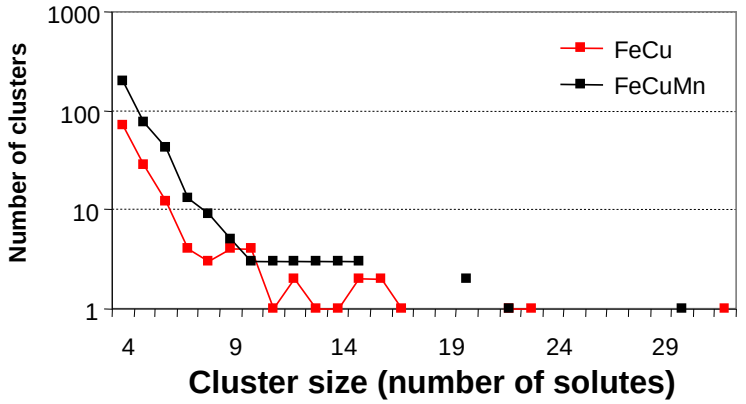

Good agreement with exp. results

(S.C. Glade et al., Phil. Mag. 85 (2005) 629.)

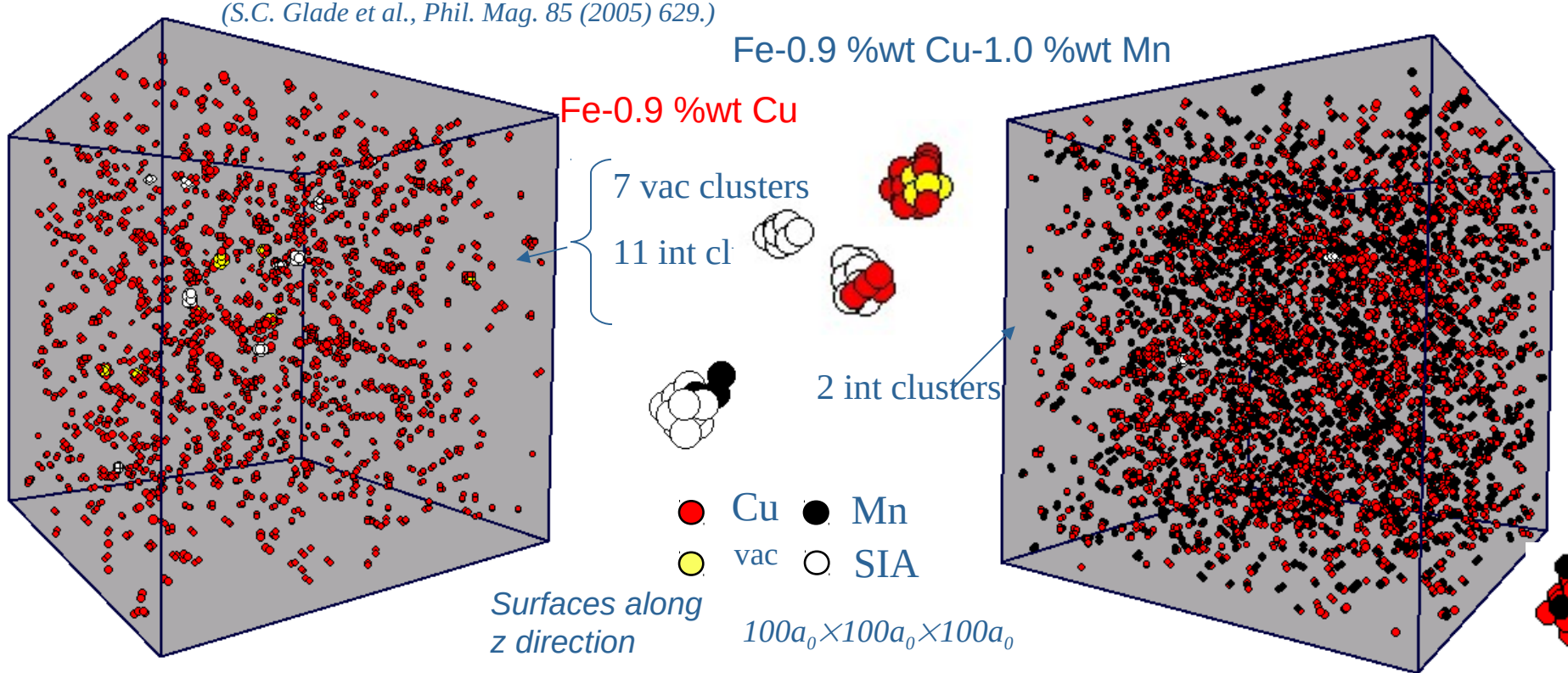

Object KMC

Objects:

- Vacancies (isolated, clustered, loops)
- Interstitials (isolated, clustered, loops)
- Solute atoms
- Traps, wells (impurities, dislocations,...)

Internal events:

- Diffusion
- Dissociation or recombination

External events (flux):

- Arrival of neutron (or ion or electron)

Follow the evolution of radiation damage: diffusion, dissociation, trapping, ...

Object KMC

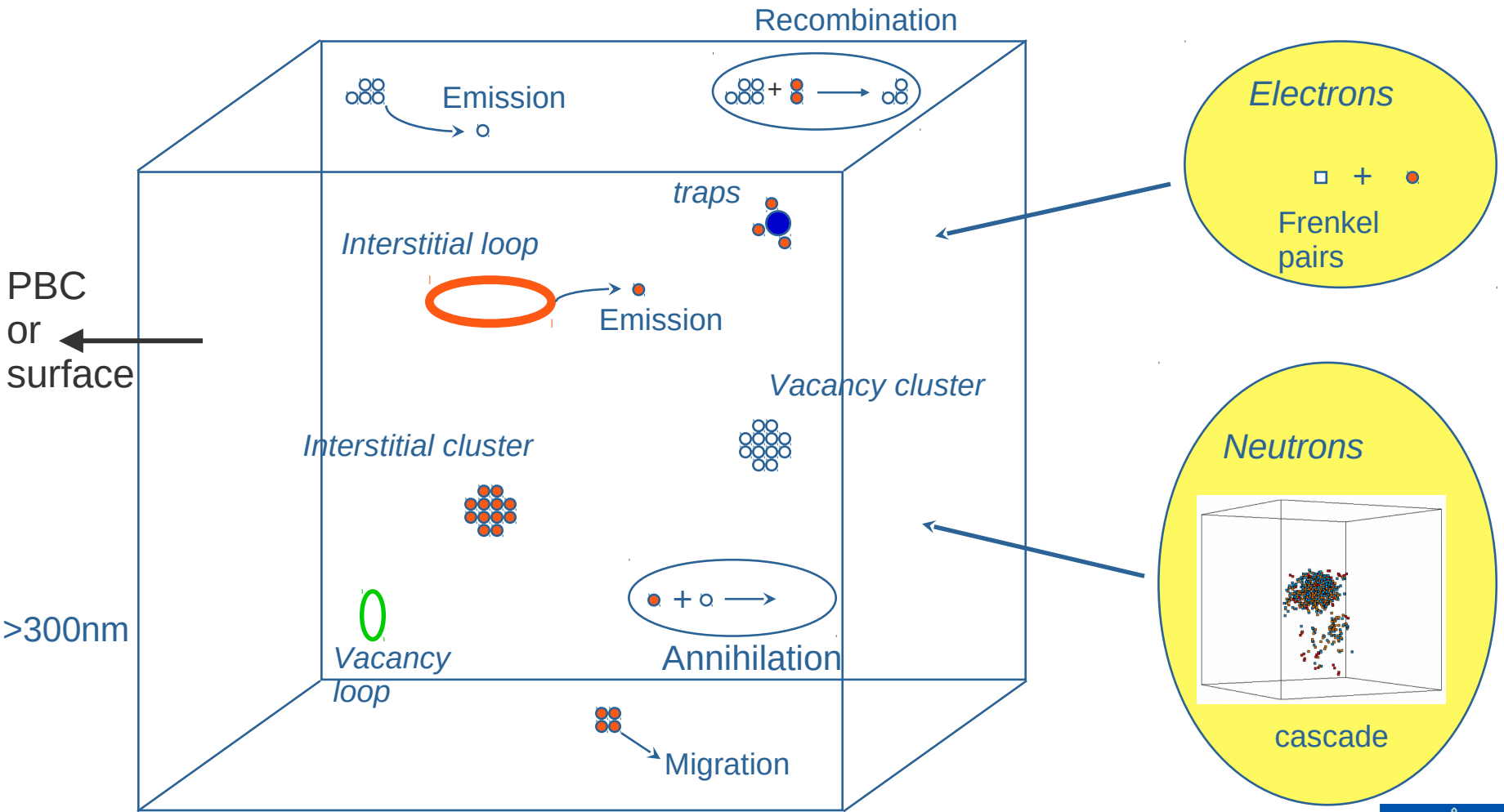
Recombination
Emission
traps
Interstitial loop
Emission
PBC
or
surface
Vacancy cluster
Interstitial cluster
>300nm
Vacancy
loop
Annihilation
Migration
Electrons
Frenkel
pairs
Neutrons
cascade

Object KMC

Interaction between two objects:

$d < R_1 + R_2$

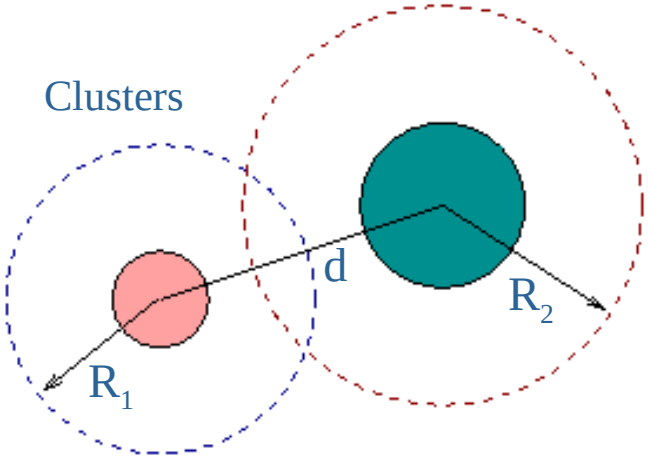

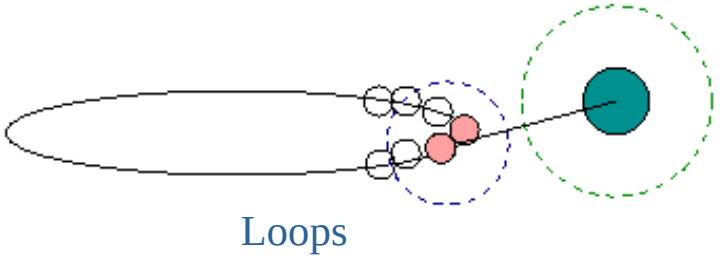

$v + i_n \leftrightarrow i_{n-1}$ + Recombination

$v + i \rightarrow 0$ + Annihilation

$i + i_n \rightarrow i_{n+1}$ + Growth of clusters

$v + v_n \leftrightarrow v_{n+1}$ + clusters

Object KMC

The choice of simulation box can significantly affect the interaction patterns.

In non-cubic boxes the interaction distance can overcome the usual cubic limitations (max one box length or infinite).

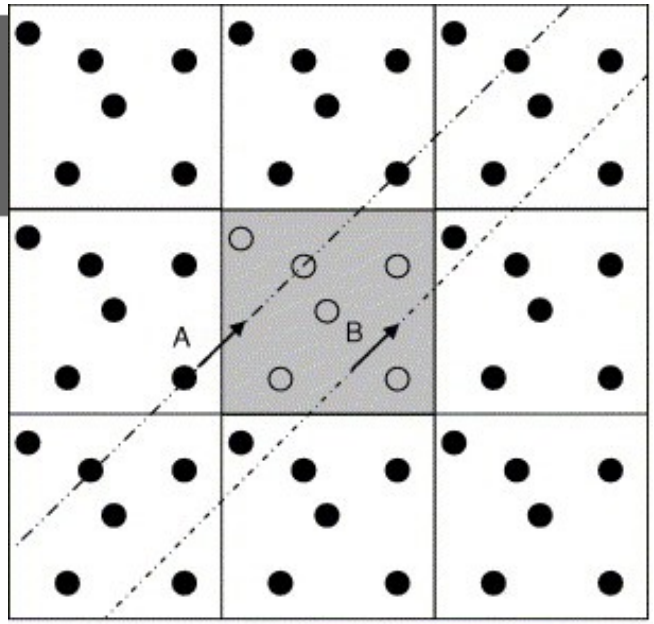

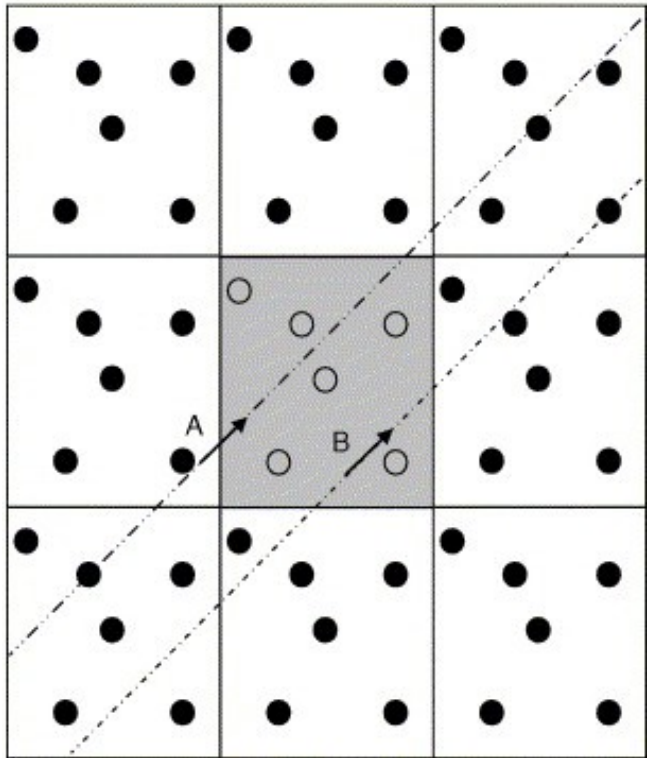

Evolution of microstructure after irradiation

Recovery of pure iron after irradiation with 3 MeV electron

Resistivity measurements, Takaki et al. 1983

close pair

I_{D2} correlated

I_E uncorrelated

II I_2 migr.

III V migr.

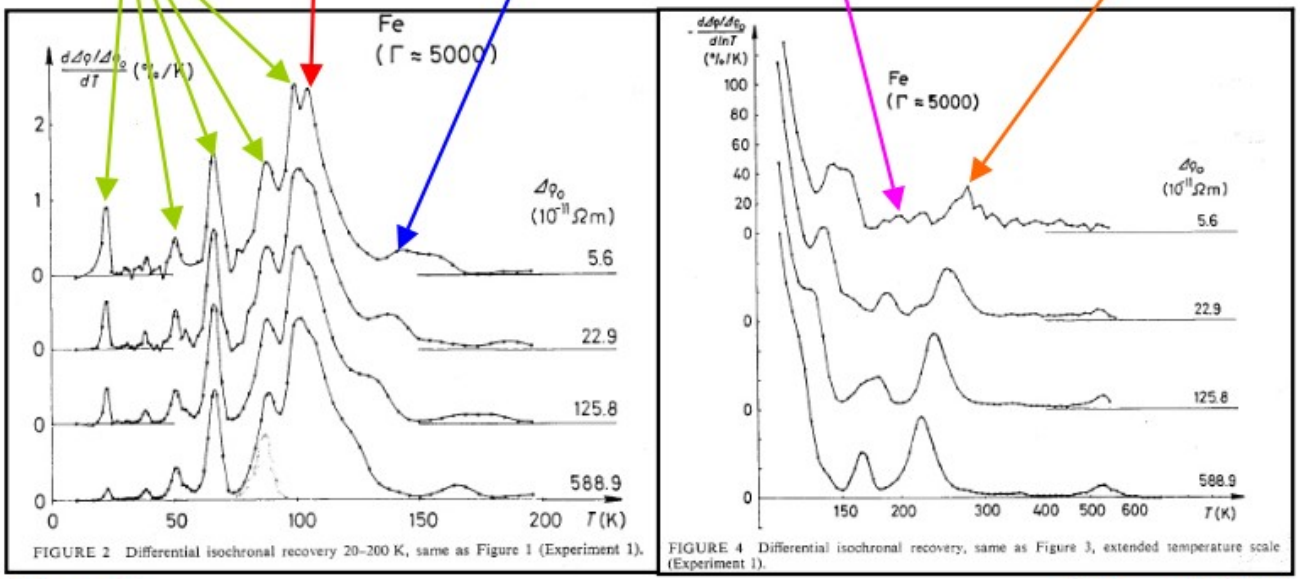

FIGURE 2 Differential isochronal recovery 20–200 K, same as Figure 1 (Experiment 1).

FIGURE 4 Differential isochronal recovery, same as Figure 3, extended temperature scale (Experiment 1).

Stage I

Stage II & III

Stage 500- 600K
only high dose

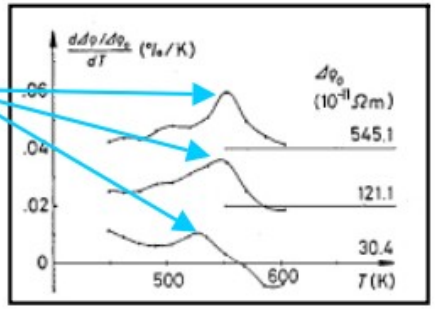

Evolution of microstructure after irradiation

Recovery of pure iron after irradiation with 3 MeV electron

Modeling : EKMC (JERK) coupled with Ab Initio calculations

J. Dalla Torre, Chu Chun Fu, F. Willaime 2003, Nature Mater.

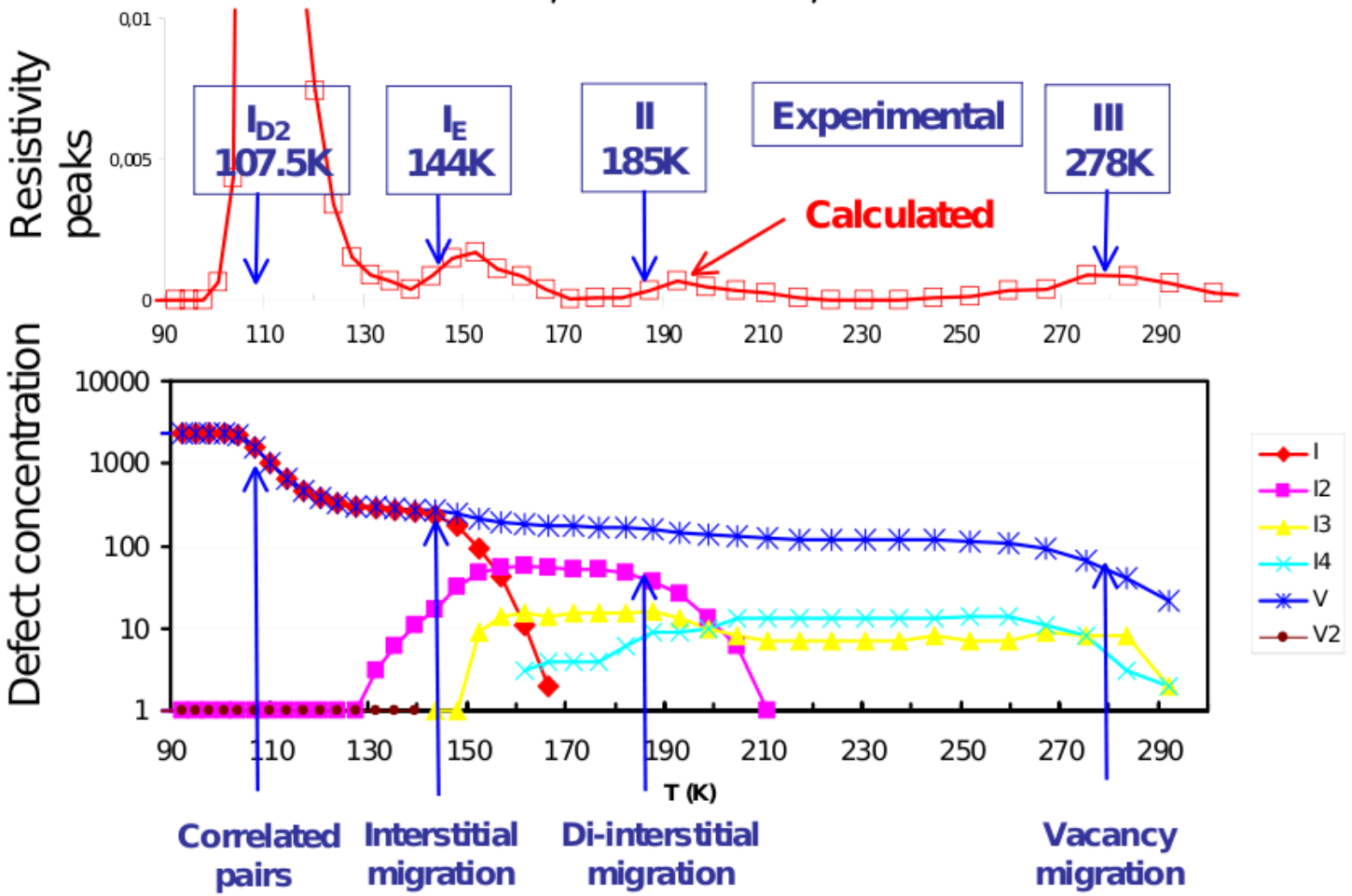

Evolution of microstructure after irradiation

Recovery of pure iron after irradiation with 3 MeV electron

Conclusions – Coupling Ab Initio-EKMC (Jerk)

- **Monte Carlo simulations in excellent agreement with measurements**
  - temperature peaks reproduced within 10 K
  - dose effects as well :
    - ✓ IE, II, III stages shift towards lower temperatures
    - ✓ 500-600K stage appears at high doses only
- **Identification/ validation of associated mechanisms**
  - confirms identification of recovery stages
    - ✓ stage 500-600K : associated with vacancy clusters dissociation
    - ✓ stage III : migration of di-vacancies improves agreement / experiment
  - confirms E_f calculations for vacancies :
    - ✓ ab initio values agree with high experimental values (2.1–2.4 eV) ; lower experimental values (1.6 eV) are incompatible : due to C-V binding E

Conclusions

We have described the basics of the Kinetic Monte-Carlo method, its implementation, difficulties and potential.

Building the rate catalouge!

Three application were discussed:

Simlations of thermal ageing of Fe-Cr alloys.

Nanostructure evolution in RPV steels.

Isochronal annealing of iron.